FATIGUE FAILURE LOAD OF LITHIUM DISILICATE RESTORATION CEMENTED ON CHAIRSIDE TITANIUM-BASE : EFFECT OF RESTORATION DESIGN

by

Peerapat Kaweewongprasert

Submitted to the Graduate Faculty of the School of Dentistry in partial fulfillment of the requirements for the degree of Master of Science in Dentistry,

Indiana University School of Dentistry, 2017.

Thesis accepted by the faculty of the Department of Prosthodontics, Indiana University School of Dentistry, in partial fulfillment of the requirements for the degree of Master of Science in Dentistry.

_____

Kamolphob Phasuk

_____

Marco C. Bottino

_____

John A. Levon

Program Director

_____

Dean Morton

Chair of Prosthodontics Department

Date _____

ACKNOWLEDGMENTS

I would first like to thank my parents, Rapeepun and Kawee Kaweewongprasert, who always give me unconditional love, care and support. I would also like to thank my beloved sister, Dr. Pennapa Kaweewongprasert, and my girlfriend, Dr. Peerapohn Taweewattanapaisan, who gave me great support no matter where they were.

In addition to my family, I would like to thank my mentors, Dr. Suteera Hovijitra, Dr. Rajapas Panichuttra, and Dr. Wallapat Santawisuk, for their belief in my potential.

I'll always be deeply grateful to my research committee members, Dr. Dean Morton, Dr. Kamolphob Phasuk, Dr. Marco C. Bottino, and Dr. John A. Levon, for their guidance, expertise and thoughtful criticism which allowed me to appreciate scientific curiosity and integrity. I also thank my research advisor, Dr. Sabrina Alves Feitosa, for her helpful suggestions during the experimental phase of the project. Thank you to Dr. Luiz Felipe Valandro for his contribution to research protocol and expert opinions. In addition to that, Mr. Eduardo Salcedo Jr. provided tremendous support by fabricating a surgical template for this project.

Thanks to my fellow Graduate Prosthodontics residents, especially Dr. Milton Revelo, who significantly contributed to and supported this project with specimen preparation and assistance running the experiment.

I would like to give thanks to Mr. George J. Eckert (IU School of Medicine) for his expertise with the statistical analysis. I am grateful for the expert opinions Dr. Jeffrey A. Platt and Dr. Wei Shao Lin contributed to this work in developing the testing protocol.

Special thanks go to Mrs. Monica Doyle for her support in organizing and coordinating the project support. This project was partially funded by material support from Dr. Shashikant Singha, of Ivoclar Vivadent, Inc., Ms. Ashley Osgood, of Straumann

Training & Education USA, Linda M. Downing, of Straumann Scan & Shape USA, and Mr. Bradley A. Cates, of Straumann USA, Teri Battaglieri, of Delta Dental Foundation.

TABLE OF CONTENTS

LIST OF ILLUSTRATIONS

INTRODUCTION

Implant supported restoration is widely accepted as one of the most predictable prosthetics treatments due to several factors, such as the proven longevity, esthetics of restoration, and high patient satisfaction.[1, 2] Although dental implant therapy is becoming more predictable, restoring implant in an esthetic zone is still highly challenging, as the clinician has to carefully look on tooth form, occlusion, mucosa contour, and restorative material.[3, 4] The implant restoration commonly consists of 3 parts: the titanium dental implant, which is osseointegrated[5, 6] to the jaw bone, the crown, and the transmucosal part, or abutment, that connects the dental implant and the crown. Nowadays, many varieties of abutments are offered by implant manufacturers. The abutment selection for each patient is dependent upon many determinants including the interocclusal space, implant angulation, and dentogingival esthetics.[7]

Conventionally, either a castable abutment or a prefabricated abutment was considered to be the preferred abutment of choice for implant restorations.[7] However, there are a couple of challenges in the restoration of these two types of abutment in an esthetic region. A patient with thin gingival phenotype may show a metal color through the facial tissue.[4, 7] The residual excess cement, especially at the interdental papilla in anterior teeth, may also result in peri-implantitis, followed by marginal bone loss.[8] In order to overcome the challenges presented by traditional abutment designs, a milled custom abutment was introduced with transmucosal features to both support a fixed dental prosthesis, as well as establish an appropriate peri-implant mucosa contour to enhance the overall prosthetic outcome.[9]

The milled custom abutment, powered by computer-aided design and computer-aided manufacturing (CAD/CAM) technology, is usually made from either titanium or

ceramic material. Titanium custom abutments represent the gold standard for restoration of a single implant due to their excellent material stability and biologic integration, with the only exception being the grayish color that may diminish the esthetic result, especially in the anterior maxillary region.[9] In order to satisfy the esthetic needs, not only the implant restoration has to be addressed, but also the surrounding mucosa has to be considered.[7] Therefore, an all-ceramic abutment made of zirconia or lithium disilicate can alternatively be used to obtain a favorable esthetic result.

Recently, a new implant restorative technique using the lithium disilicate material connected with the titanium-base was introduced.[10-12] The lithium disilicate restoration can either be fabricated to full contour anatomy, connected to the titanium-base, or fabricated as a cutback anatomical structure and connected with titanium-base, which is then clinically cemented with another lithium disilicate crown.[13] These combined abutment solutions allow the clinician to fabricate either milled customized screw-or cement-retained restorations with high esthetics value and lower cost when compared to conventional abutments.[11] In addition, the process of laboratory fabricated custom abutment and implant restoration can take up to 10-14 days after implant impression. By using the chairside Computer-Aided Design and Computer-Aided Manufacturing (CAD/CAM) technology (e.g. CEREC- Chairside Economical Restoration of Esthetic Ceramics system), single implant restoration can be fabricated in-house in a very short time and delivered to the patient within a day of implant impression.[11]

There are several designs of all-ceramic restoration to achieve an esthetic outcome for restoring the implant in an anterior maxillary area. Previous studies[14-18] have been mainly focused on the performance of the zirconia abutment, but there were only a

few studies that had investigated the mechanical properties, including fatigue behavior of lithium disilicate connected with the chairside titanium-base in different designs. Therefore, the present study aims to investigate the fatigue resistance of different designs of lithium disilicate restorations fabricated by chairside CAD/CAM milling technique (CEREC) connected to titanium-base by using the dynamic fatigue loading test. The null hypothesis of this study was that no statistically significant difference in fatigue resistance among various designs of all-ceramic material connected with the chairside titanium-base.

REVIEW OF LITERATURE

Two systematic reviews presented that implant-supported single-crowns are a practicable alternative to traditional fixed dental prosthesis (FDPs) for single-tooth replacement.[19, 20] In a meta-analysis of these studies, a survival rate of 96.8% for implants supporting single-tooth crowns and 94.5% for single crown supported by implants after an observation period of at least 5 years were reported.[20] Furthermore, the estimates of the survival proportion after 5 years were 91.2% (95% CI: 86.8–94.2%) for the implant that supported all-ceramic crowns.[20] In 1981, Gibbs et al. used a sound transmission system for measuring chewing force and reported an average mastication force in natural dentition at 720 N.[21, 22] In particular for anterior region were in the range of 150–235 N with an average of 206 N.[23, 24] It was also documented that lithium disilicate restoration cemented on solid titanium and zirconia abutments demonstrated sufficient resistance to withstand normal chewing forces.[25]

Both an excellent survival rate of implant and restoration, as well as the dentogingival esthetics have tremendous influence on patient satisfaction. The dentogingival esthetic consists of the appearance of the restoration and gingival tissue around the implant. Furhauser R. et al. and Belser UC. et al.[26, 27] introduced the pink esthetic score (PES) and white esthetic score (WES) for describe the esthetic for single implant restoration more objective. Furthermore, Sailer I. et al. indicated the crucial factors for restoring implants in an esthetic area, which included the choice between cementation and screw retention, the position and angulation of the implant, and the thickness/scalloping of the surrounding mucosa. An in vitro study concluded that the type of abutment or crown material and the gingival thickness have significant influence on color changes of the mucosa. Moreover that zirconia induces the least noticeable color

changes to the mucosa.[7]

Zimbic et al. reported the 5-year survival rates, the technical and biological complication rates of zirconia and titanium abutments in canine and posterior regions of the mouth. It was shown that there was no statistically significant different between zirconia and titanium.[28] Zirconia then become more popular as material of choice for implant restoration in the anterior area due to its superior optical property as compared with titanium.[28-30] Even with its remarkable optical property, several authors reported clinical failures of one-piece zirconia abutments, where the entire abutment is made from zirconia, because of its mechanical disadvantage.[14-18]

Several in vitro studies[13, 31, 32] have shown exceptional mechanical performance, including fractural strength and stiffness of the titanium-base combined with ceramic restoration. Recently, Elsayed A. and colleagues described that the lithium disilicate abutments and crowns indicate foreshadowing durability and strength after long-term fatigue loading. The authors also concluded that the use of a titanium-base combined with all ceramic material improved the strength of the restoration.[12] In addition, a case report also presented the use of a titanium-base combined with ceramic restoration designs. These specific designs have been extensively used with the CEREC system, which allows the clinician to complete both cement-and screw-retained restorations in a day.[11]

The International Organization for Standardization (ISO14801: 2007 Dynamic Fatigue Test for Endosseous Dental Implants) recommended testing a single, endosteal, and transmucosal dental implant under a worst-case scenario. The marginal bone loss of 3.0 mm ± 0.5 mm from the nominal bone level is applied to represent the worst-case application. In addition, the specimen holder is also specified to have a modulus of

elasticity higher than 3 GPa, which will not deform the test specimens.[33] Nevertheless, Kelly R. et al. claimed that this embedment material has an appropriate elastic modulus for a bone analog material (approximately 20 GPa), is easily machined, and is sufficiently tough for cyclic testing.[34] ISO also recommended either wet (37 °C ± 2 °C) or dry (20 °C ± 5 °C) test environments. In addition, the loading frequency shall be no more than 15 Hz.[33] In contrast, Fraga S. et al. pointed out the relative time consuming factor in fatigue loading of all-ceramic restoration. The authors specified that fatigue strength was not different among frequencies 2, 10 and 20 Hz in zirconia discs. The study suggested using up to 20 Hz in order to accelerate fatigue strength tests.[35] One of the methods used to run a fatigue test is a stepwise protocol, used to forecast clinical mechanical limits, because of the differences of the extreme non-physiological conditions placed on the materials. The stepwise protocol stimulates the failure of the restoration under fatigue circumstances at different cycles. First, it warms-up the load of specimens for the specified number of cycles. Next, it steps up evenly until reaching the upper limit of the testing.[35, 36] Several studies[36-38] also utilized stepwise protocol to test dental restoration in order to stimulate the mastication force in the oral environment.

MATERIALS AND METHODS

All materials and instruments used in this experiment are listed in Table I. This study consisted of 3 groups (N=10/each): lithium disilicate crowns cemented on titanium custom abutment (CTD); full contour monolithic lithium disilicate crowns bonded to the titanium-base **(**VMLD); and lithium disilicate crowns cemented on lithium disilicate customized anatomic structures and cemented to the titanium-base (VCLD) (Table II, Figure 1 and 2). Groups CTD and VCLD customized anatomic structures, designed and fabricated following manufacturer's recommendations. Preparation guidelines for lithium disilicate restoration were 2.0 mm incisal reductions, and 1.0 mm axial reductions with a deep chamfer margin circumferentially. For Group VMLD, full contour monolithics were cemented on titanium-base. The various designs of lithium disilicate restorations cemented to the abutments were considered as a combined restorative complex, which defined the groups.

Specimen holder fabrication and implant embedment

An epoxy resin-glass fiber composite (NEMA Grade G-10, Piedmont Plastics, Cincinnati, OH), which had the elastic modulus of 18.62 GPa, was cut into square blocks (30 × 30 × 30 mm). All 30 implant fixtures were placed into a specimen holder and embedded into NEMA G-10 [34]. A surgical template (Figure 3) was designed on AutoCAD software (Autodesk, Inc., USA) and 3D printed with standard clear resin from FormLab2 Printer (Formlabs, Inc., USA). Afterward, the surgical template was agitated in isopropyl alcohol (IPA) for 30 seconds and soaked for 10 minutes. Then the surgical template was light cured under UV light box at 405 nm wavelength light sources for 24 hours. Lastly, a metal sleeve for Straumann® Guided Surgery (Straumann® LLC,

USA) was fitted to the prepared hole on the surgical template (Figure 4).

A pilot drill 2.2 mm × 36 mm, twist drill 2.8 mm × 36 mm, and twist drill 3.5 mm × 36 mm, guided profile drills bone level 4.1 mm × 37 mm, guided taps for bone level 4.1 mm × 42 mm, one dot (2.2, 2.8, and 3.5 mm) drill handle, and C handle H-4 from Straumann® bone level guided surgical kit (Straumann® LLC, USA) were used respectively to prepare the channel along with the drill press machine and surgical template (Figure 5). A depth of 7 mm channels was drilled on the specimen holder utilizing the same surgical template throughout the experiment. The marginal bone loss of 3.0 mm ± 0.5 mm from the nominal bone level was applied.

In the end, all bone-level threaded cylindrical implants (Straumann® Bone Level Implant, SLA surface, RC 4.1 × 10 mm, Straumann® LLC, USA) were embedded into NEMA G-10 block through a surgical template with implant driver and manual torque wrench. The timing of the implant was controlled by lining up the flat surface on the implant mounted to the red line on surgical template. The insertion torque value was tested with the manual torque wrench to be greater than 35 Ncm. All of the tested specimens were randomly labeled and numbered.

Specimen fabrication

The total of 20 left maxillary anterior incisor group VCLD and VMLD restorations were virtually designed utilizing computer software (CEREC 4.4 Software, Sirona Dental Systems LLC, USA) and fabricated with milling technology (Sirona CEREC® inLab MC XL, Sirona Dental Systems LLC, USA) according to the specific design. All lithium disilicate material for monolithic restorations and crowns were made

from IPS e.max CAD LT block, while customized anatomic structures were made from IPS e.max CAD MO block. The titanium-base were made using RC Variobase® for CEREC®.

All the pre-crystallized state specimens were finished from the block using a diamond-separating disc (Figure 6-7). Then they were carefully placed on the titanium-bas. The fit was checked by observing the position of the rotation lock. The pre-crystallized state specimens were pre-polished with a diamond rubber polisher, fine polished with a high-gloss rubber polisher, high-gloss polished with brushes, and polishing paste (Figure 8-9). The pre-crystallized state specimens were cleaned with ultrasonic in deionizing water for 3 minutes, rinsed, and oil free air-dried. Afterward, the pre-crystallized state specimens were fixed in the center of the crystallization tray with IPS Object Fix Putty in Programat CS (Ivoclar Vivadent®, USA) furnace (Figure 10-11, 13). According to manufacturer's recommendations, the IPS e.max LT block was fired under program 1 IPS e.max CAD Crystallization/ Glaze (Figure 12). The IPS e.max MO block was fired under program 7 IPS e.max CAD Crystallization/ Glaze (Table III).

The crystallized customized anatomic structure specimen was scanned and replicated to custom titanium abutment and crown using 7 series Straumann powered by Dental Wings desktop scanner, Straumann® CARES® Visual 10.3 software. A total of 10 custom titanium abutments and crowns were fabricated from Straumann® milling center (Straumann® LLC, Arlington, TX). Then all crystallized lithium disilicate crown were carefully checked on the custom titanium abutments (Figure 14).

Preparation of titanium-base

For Groups VMLD and VCLD, the titanium-base was connected to an implant analog by tightening the basal screw hand-tight. Then, monolithic crown and customized anatomic structures were placed on titanium-base and the relative position of the component was marked with waterproof pen (Figure 14). Silicone fast set was used to protect the emergence profile and the screw channel of implant analog. The titanium-base was blasted with aluminum oxide particles, 50 μm, 2 bars, 10 mm in distance, 10 seconds or until a matte surface was achieved (Figure 15). Subsequently the abutment was steamed, air-dried and a thin coat of silane was applied for 60 seconds (Figure 16-17). Lastly, the screw channel was protected with Teflon tape.

Surface treatment protocol

For Group VCLD, the customized anatomic structure was cleaned in an ultrasonic unit for 3 minutes. Then the intaglio surface of screw channel was etched with 5% HF for 20 seconds, rinsed with deionized water for 60 seconds, ultrasonically cleaned for 5 minutes, air-dried, and silanized for 60 seconds. After bonding between the titanium-base and the customized anatomic structure is completed, the bonding interface of the customized anatomic structures was prepared with similar protocol as was the intaglio surface (Figure 20).

The CTD crowns, VMLD crowns, and VCLD crowns were cleaned in an ultrasonic unit for 3 minutes. The intaglio surface was etched with 5% HF for 20 seconds, rinsed for 60 seconds to remove the acid, ultrasonically cleaned for 5 minutes, air-dried, and silanized for 60 seconds.

Bonding and sterilization protocol

For Group CTD, the custom titanium abutments and Regular Cross-fit (RC) basal screws were autoclaved with moist heat at 134 °C / 273 °F for 18 minutes (Midmark M11 UltraClave automatic sterilizer, Midmark CORP, USA). Afterwards, the custom titanium abutments and RC basal screws were connected on dental implants embedded in the specimens holder and torqued up to 35 Ncm using a manual torque wrench. The manual torque wrench was calibrated and secured after each use. Each abutment screw was re-torqued to a final torque value of 35 Ncm after 10 minutes from initial torque. The abutment access channel was protected with Teflon tape 2 mm from the top of the palatal surface. The screw channel was filled with implant channel filling material (Telio CS Inlay Universal). The Telio CS inlay Universal was polymerized with a Light Emitting Diode (LED) curing light (Bluephase 20i, Ivoclar Vivadent®, USA) under high power mode for 10 seconds (light intensity > 650 mW/cm^2). The LED curing light was calibrated with a visible curing light meter (Cure Rite®, Dentsply Caulk, Milford, DE) before use. All surface treated crowns were cemented to the titanium abutments with resin cement. The excess luting agent was removed with a microbrush. Glycerine gel was then applied at the crown margin. A load of 300 grams was applied on the incisal edge until the completion of auto-polymerization (8 minutes start from mixing) to ensure the film thickness. After the completion of auto-polymerization, the glycerine gel was rinsed off with deionized water.

For Group VMLD, a thin layer of resin cement was directly applied from the mixing syringe to the bonding surface of the titanium-base and the intaglio surface of the monolithic crown. Both components were connected, and the position markings were

aligned. Excess of the resin cement was removed using a microbrush. Then, glycerine gel was applied at the crown margin. The specimens were held immobile with diamond-coated tweezers until the completion of auto-polymerization, which was 8 minutes start from mixing. After the completion of auto-polymerization, the glycerine gel was rinsed off with deionized water. The Teflon tape was removed and excess luting agent cleaned with a microbrush. The combination of the titanium-base and monolithic crown were autoclaved with moist heat at 132 °C / 270 °F for 3 minutes in an automatic sterilizer.

Afterwards the combination of the titanium-base, monolithic crown, and basal screw were connected on dental implants embedded in the specimen holder in a similar fashion to the CTD group, except that the rest of the channel was filled with resin composite. The resin composite was polymerized with a LED curing light under high power mode for 10 seconds (light intensity > 1000 mW/cm^2).

For Group VCLD, a thin layer of resin cement was directly applied from the mixing syringe to the bonding surface of the titanium-base and the intaglio surface of customized anatomic structures. Both components were cemented in such a way that the position markings were aligned (Figure 18). The excess of the resin cement was removed using a microbrush. Then, glycerine gel was applied at the crown margin. The specimens were held immobile with diamond-coated tweezers until the completion of auto-polymerization. After the completion of auto-polymerization, the glycerine gel was rinsed off with deionized water. The Teflon tape was removed and excess luting agent cleaned with a microbrush. The combination of the titanium-base and customized anatomic structures were autoclaved with moist heat at 132 °C / 270 °F for 3 minutes in an automatic sterilizer (Figure 19). Afterwards the combination of titanium-base,

customized anatomic structures and basal screw were connected on dental implants embedded in a specimen holder in a similar fashion to the CTD group (Figure 21-22).

All surface treated crowns were cemented to the customized anatomic structures with resin cement (Figure 23). The excess luting agent was removed with a microbrush (Figure 24). Then, the glycerine gel was applied at the crown margin. The specimens were subject to 300 grams of load on the incisal edge until the completion of auto-polymerization (Figure 25). After the completion of auto-polymerization, the glycerine gel was rinsed off with deionized water.

Specimen storage

All specimens were soaked under deionized water in the 37 °C incubator for 24 hours before testing (Figure 26).

Stepwise protocol

Dynamic fatigue testing of dental implants was performed based upon ISO 14801:2007. All specimens were positioned at 38 ± 2 degrees to the long axis of the prosthesis as shown in Figures 27 and 28. The universal testing machine (Instron ElectroPuls E3000, Instron Corporation, Norwood, MA, US, Figure 1) was calibrated before start of the measurements and run by a well-trained operator. Fatigue loading test was run in dry conditions at room temperature (20 °C ± 5 °C). The load was applied using a stainless-steel round tip (10 mm in diameter), which was centrally located at the palatal surface 1 mm from the incisal edge. A repositioned device was made of clear custom tray material (Triad® TruTray™ VLC, Dentsply Intl, USA) and clear vacuum

sheet to insure a reproducible position of the stainless steel-round tip (Figure 29). The position was double checked with the reposition device and a double-sided articulating film (AccuFilm® II, Parkell, Inc., Edgewood, NY) before each test. Once the position was confirmed, double-sided tape and transparent film were attached to the palatal surface of the specimens to facilitate even force distribution. Cyclic loading was programed by BlueHill version 2.0 software (Instron Corporation, Norwood, MA, US) and applied at 20 Hz,[35] starting with a load of 100 N for 5000 cycles for preconditioning the specimens, followed by 200 N for 30,000 cycles in the first step. The compressive load was then staged at 400, 600, 800, 1000, 1200, and 1400 N at a maximum of 30,000 each cycle. All specimens were tested until either a catastrophic failure or the maximum of 215,000 cycles was reached.[37] In the event that the specimen passed 1400 N; it was documented as the maximum load and cycles. Initial failure was described as any implant deformations, abutment screw deformations, abutment deformations, crack or craze line on ceramic structure, prior to catastrophic failures. Catastrophic failure was defined as the fragmentation of any components.

Fracture analysis

All specimens were examined initially and reevaluated at the end of each load under optical microscope Leica MZ 125 (Leica Microsystems GmbH, Wetzlar, Germany) at 5 × magnification and with a digital camera (Canon EOS Rebel T3, Canon INC, USA) (Figure 30-35). The integrated Leica DFC290 HD (Leica Microsystems GmbH, Wetzlar, Germany) digital camera and Leica Application Suite software (Leica Microsystems GmbH, Wetzlar, Germany) were used to record and analyze both initial and catastrophic

failures. Different magnifications, ranging from 0.8 × to 10 ×, were utilized to detect the different characteristics of each failure feature.

Statistics analysis

ANOVA was done using SAS version 9.4 (SAS Institute Inc., Cary, NC). The survival analysis was done in R 3.3.2 (R Core Team 2016, Vienna, Austria) using the survival package version 2.38 (Therneau T 2015) survfit and survreg functions.

Group comparisons were made using one-way ANOVA followed by pair-wise comparisons if the overall group effect was statistically significant. The study was designed to have 80% power to detect a difference of 152 N for maximum force between any two groups. In addition to the ANOVA, Kaplan-Meier survival plots and Weibull survival analyses were performed. A 5% significance level was used for all tests.

RESULTS

For the initial failure load, VCLD was significantly lower than CDT ($p < 0.05$) and VMLD ($p < 0.05$), but CDT and VMLD were not significantly different from each other. Survival probability using the Kaplan−Meier and Weibull model of initial failure is illustrated in Figure 36. For catastrophic failure load, VMLD was significantly higher than CDT ($p < 0.05$) and VCLD ($p < 0.05$), but CDT and VCLD were not significantly different from each other. Survival probability using the Kaplan−Meier and Weibull model of catastrophic failure is illustrated in Figure 37. Apart from that, the total number of cycles of VMLD was significantly higher than CDT ($p < 0.05$) and VCLD ($p < 0.05$), but CDT and VCLD were not significantly different from each other. Survival probability using the Kaplan−Meier and Weibull model of total cycles is illustrated in Figure 38.

Table IV shows both initial and catastrophic failure loads, as well as the number of cycles. In addition, the Weibull characteristic strength and modulus is presented in Table V. VMLD's Weibull modulus is higher than the other two groups, showing a small variation between specimens. Mode of failure at catastrophic failure load is presented in Table VI. There were two VMLD specimens that survived the fatigue test beyond 1400 N and 215,000 cycles. Observation of the initial failure of each specimen showed multiple modes of failure. One of the VMLD specimens that survived the fatigue test presented implant deformation, while the other one initiated a crack line on the lingual aspect. The VMLD cracked specimen was always associated with screw channel on lingual aspect and titanium-base (Figure 39). One of VCLD specimens showed a crack line on the lithium disilicate customized anatomical structure and crown at higher loads (Figures 40 and 42). Furthermore, most of the failure from group CTD presented the fracture of lithium disilicate crown (Figures 43 and 44).

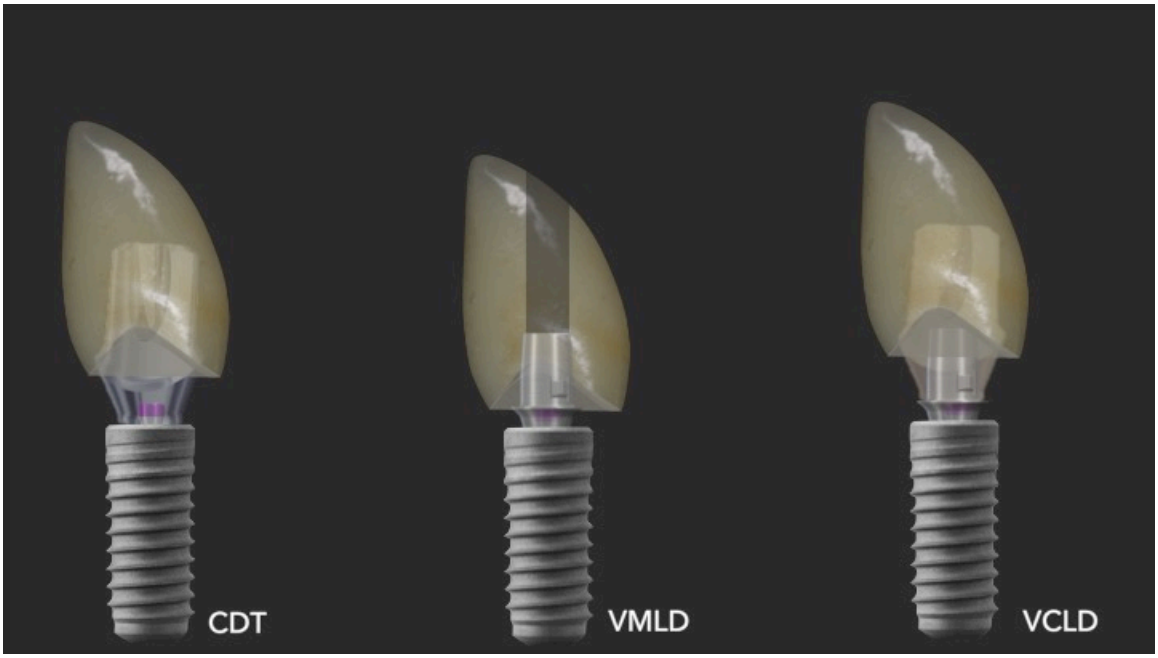

FIGURE 1.

Three different groups of abutment and crown design

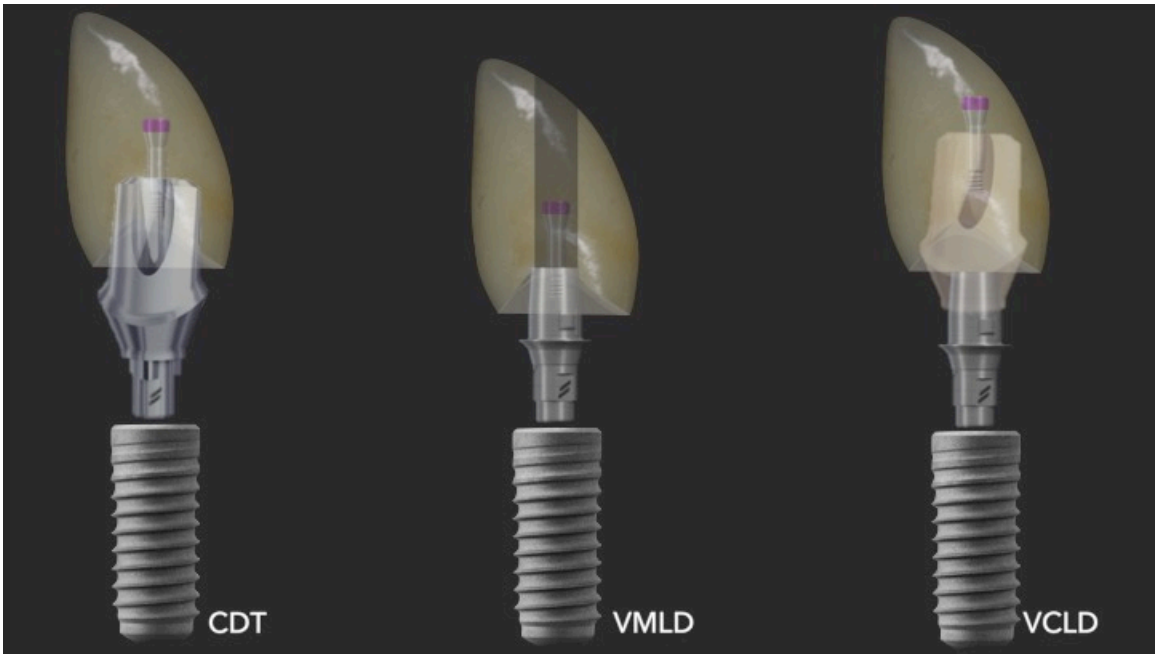

FIGURE 2.

An assembly of all components of abutment and crown in three different design groups

CTD: E.max CAD crowns bonded to Straumann® CARES titanium custom abutment

VMLD: Full contour monolithic e.max CAD crowns bonded to the Variobase® for CEREC® abutment

VCLD: E.max CAD crowns without access hole bonded to Variobase® for CEREC® abutment and zirconia customized structure

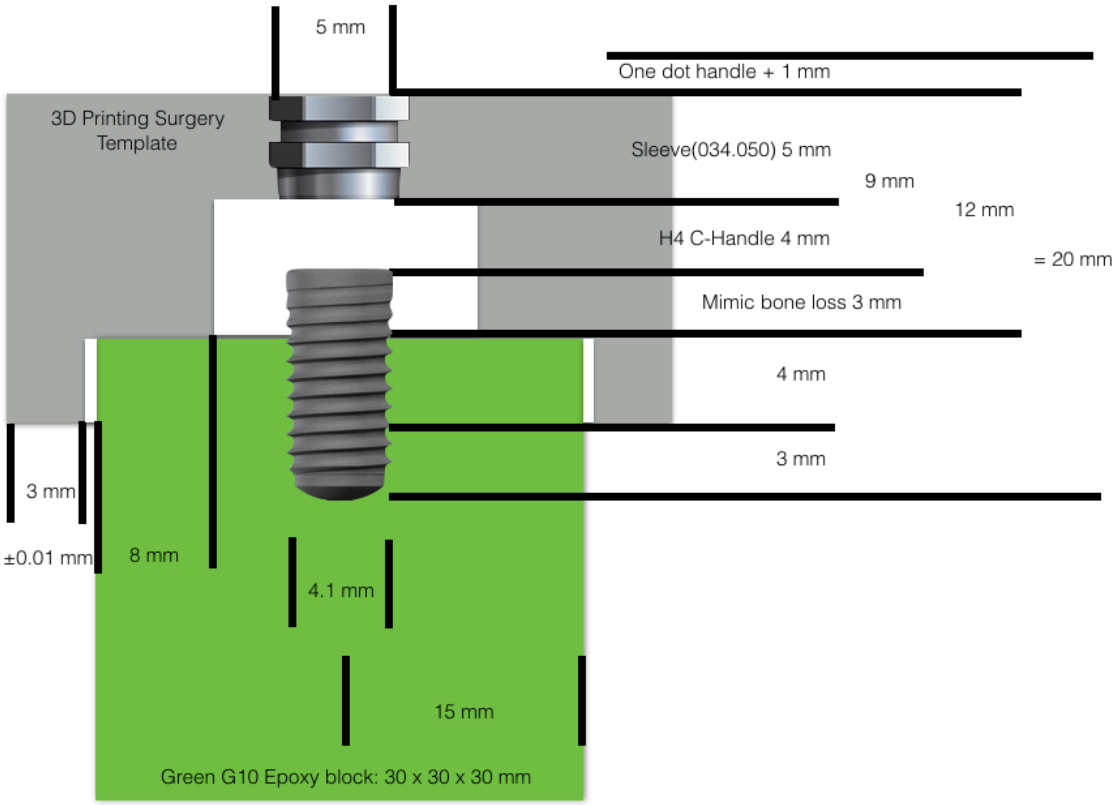

FIGURE 3.

The design of surgical template and implant position related to specimen holder.

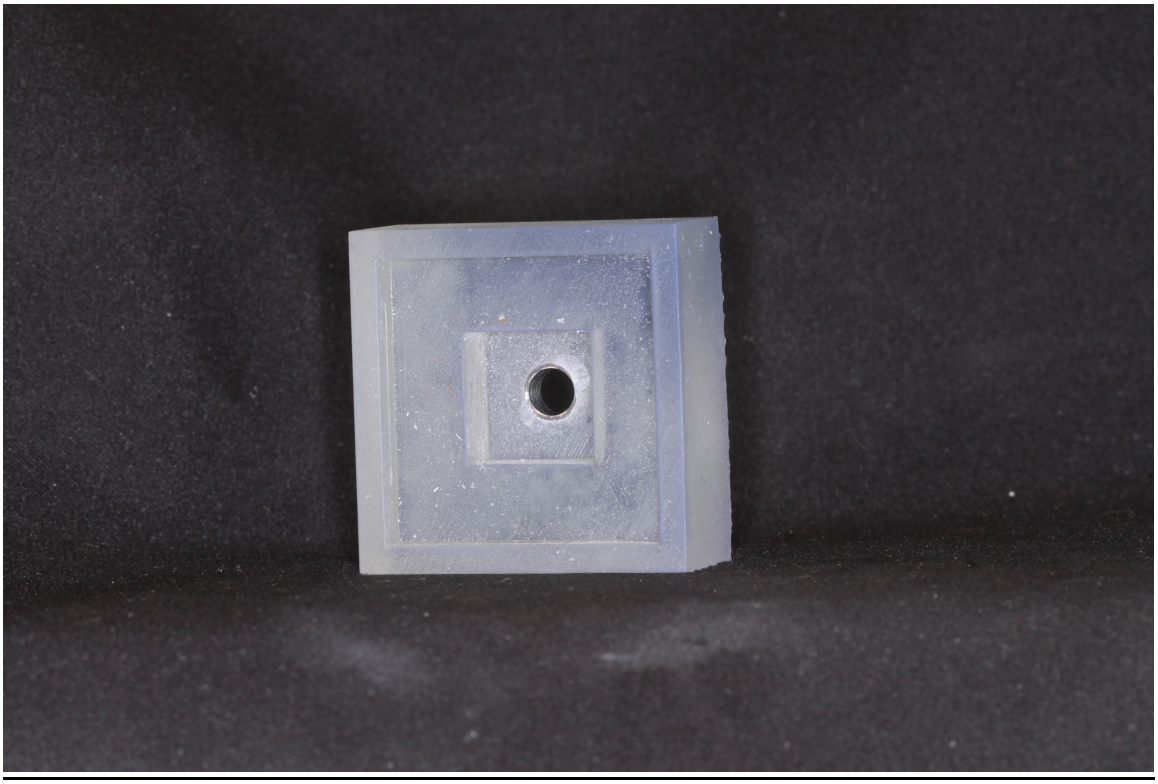

FIGURE 4.

The 3D printed surgical template

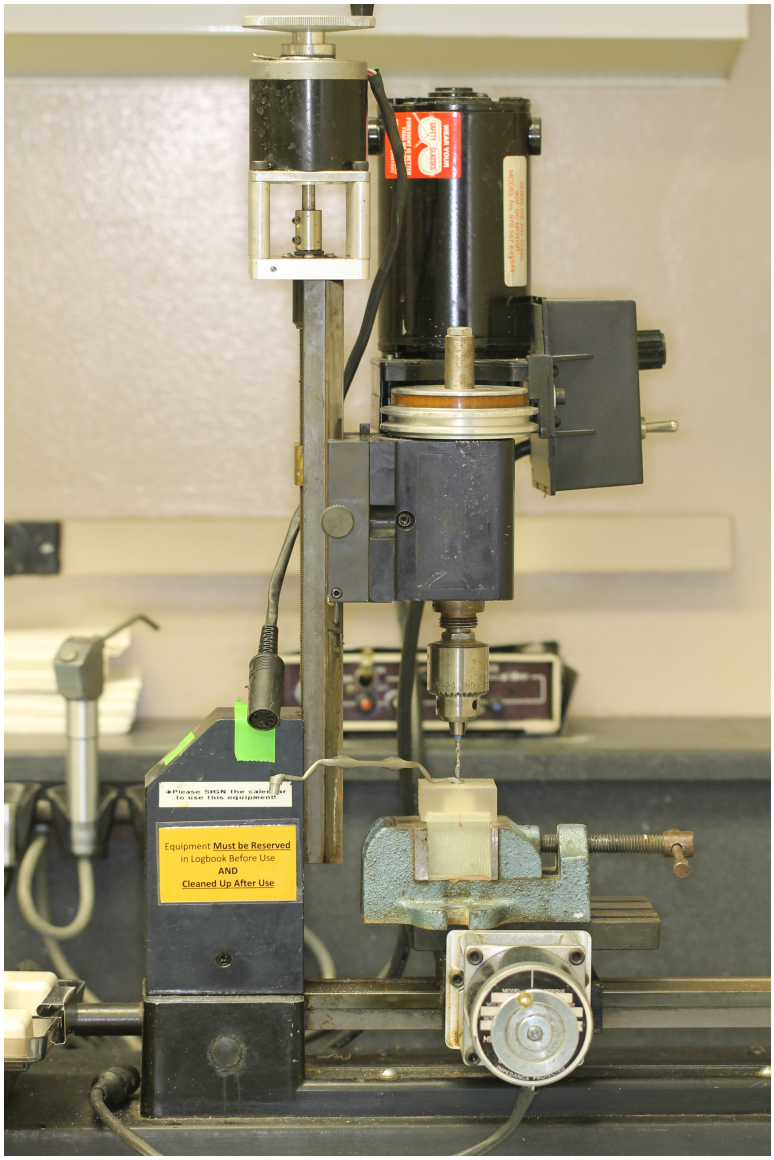

FIGURE 5.

The implant channel preparation utilizing the drill press machine and surgical template

FIGURE 6.

The pre-crystallized state specimens

FIGURE 7.

The pre-crystallized state specimens were finished from the block using a diamond-separating disc.

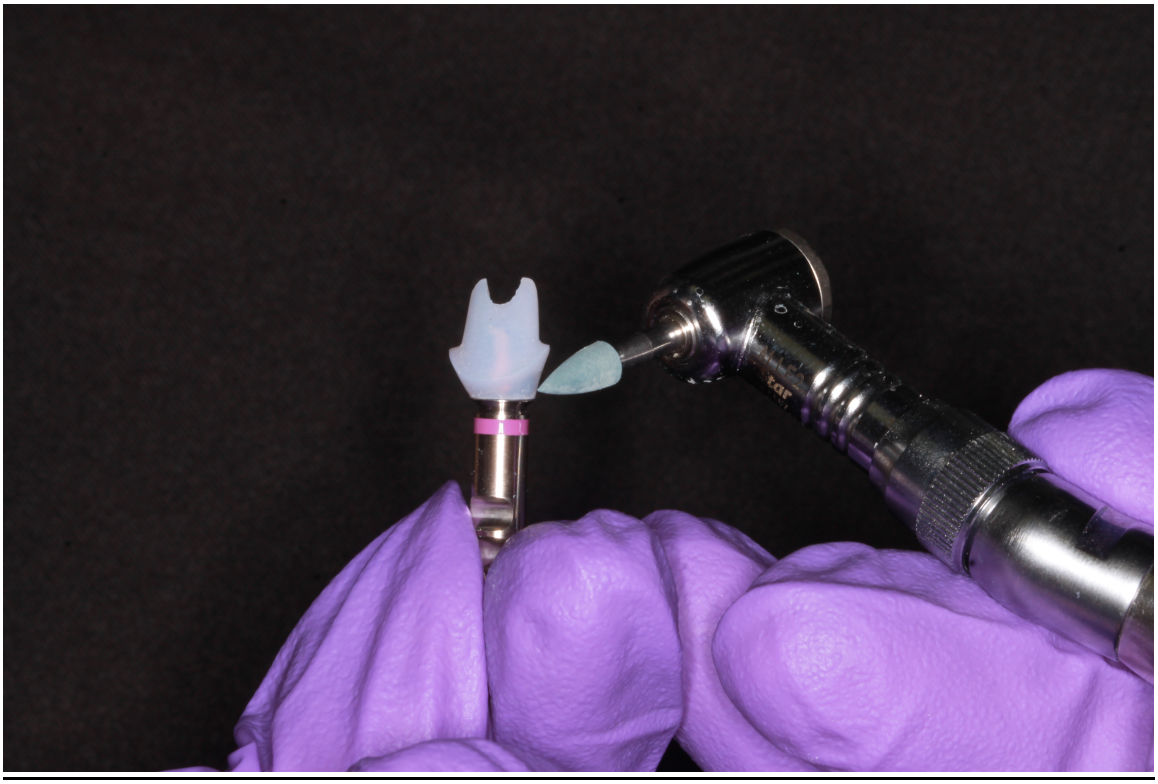

FIGURE 8.

The pre-crystallized state specimens were pre-polished with a diamond rubber polisher.

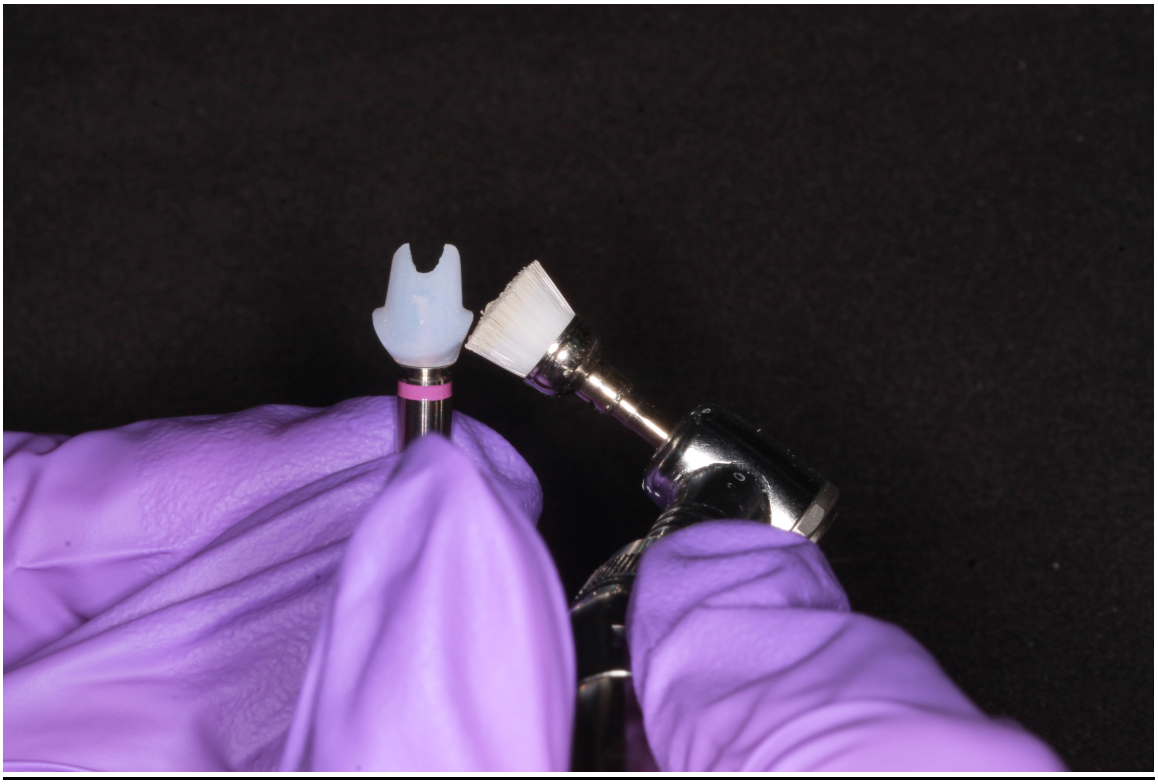

FIGURE 9.

The pre-crystallized state specimens were pre-polished with high-gloss polished with brushes, and polishing paste.

FIGURE 10.

The pre-crystallized state specimens were fixed with IPS Object Fix Putty.

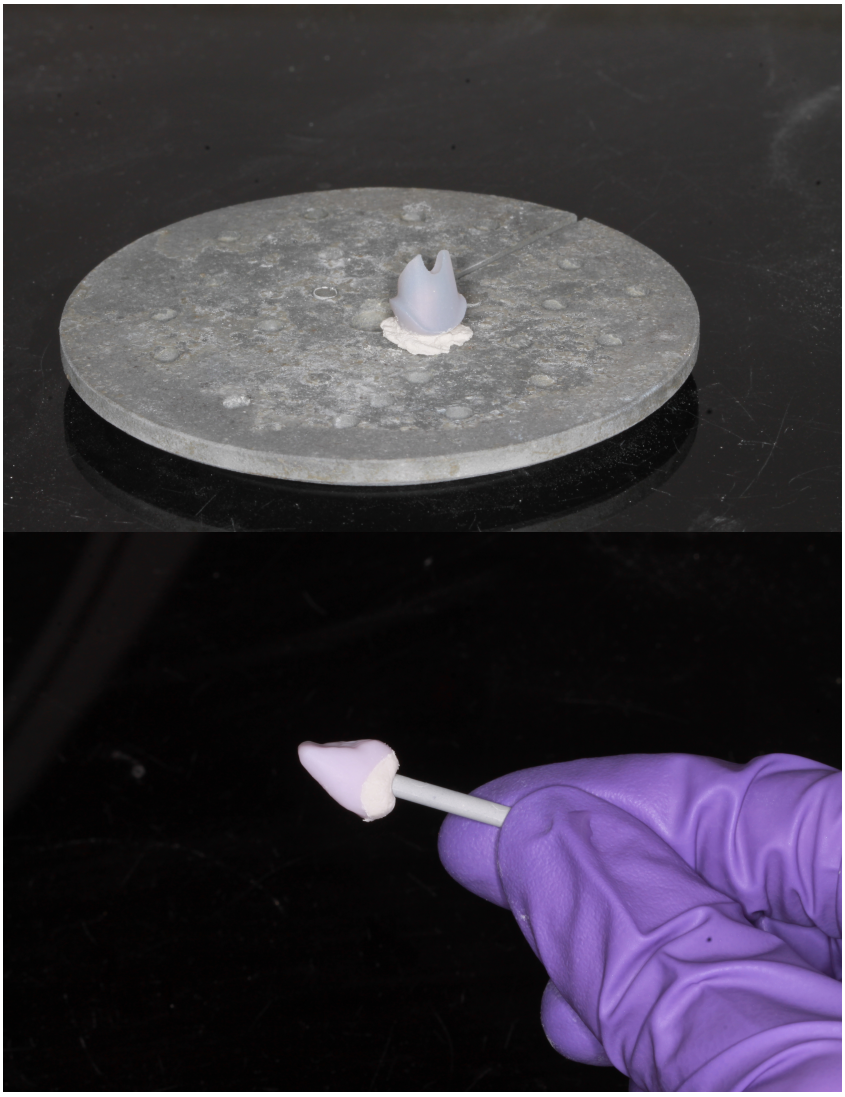

FIGURE 11.

The pre-crystallized state specimens were fixed the in the center of the IPS e.max CAD crystallization tray.

FIGURE 12.

The pre-crystallized state specimens were fired in Programat CS furnace.

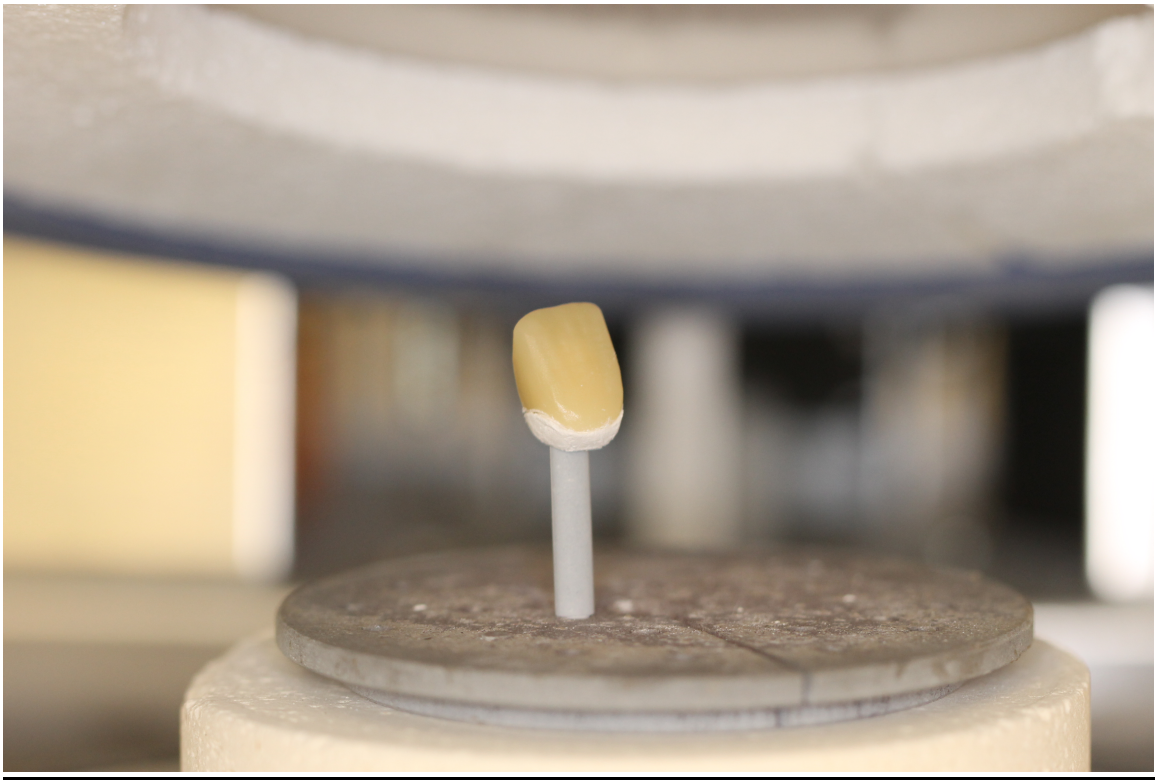

FIGURE 13.

The post-crystallized state specimens were fired in Programat CS furnace.

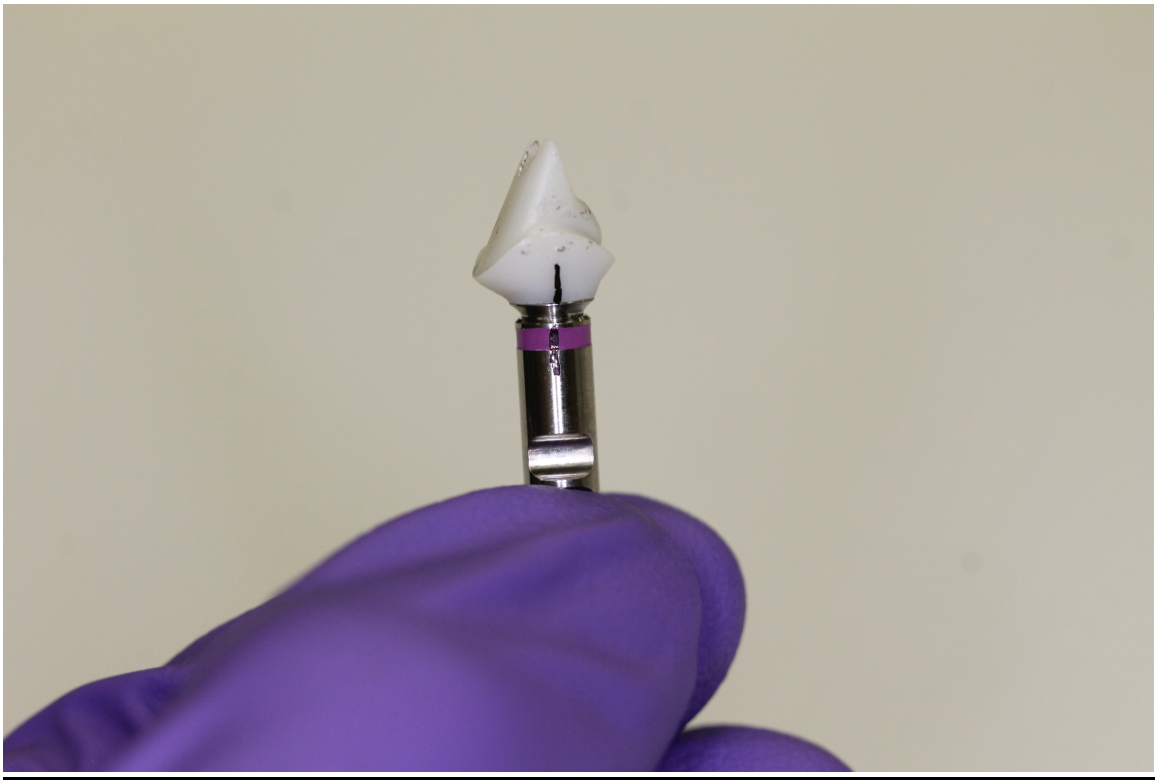

FIGURE 14.

The customized anatomic structures were placed on titanium-base and marked the relative position of the component with waterproof pen.

FIGURE 15.

The titanium-base was blasted with aluminum oxide particles.

FIGURE 16.

The titanium-base was streamed.

FIGURE 17.

The titanium-base was applied silane for 60 seconds.

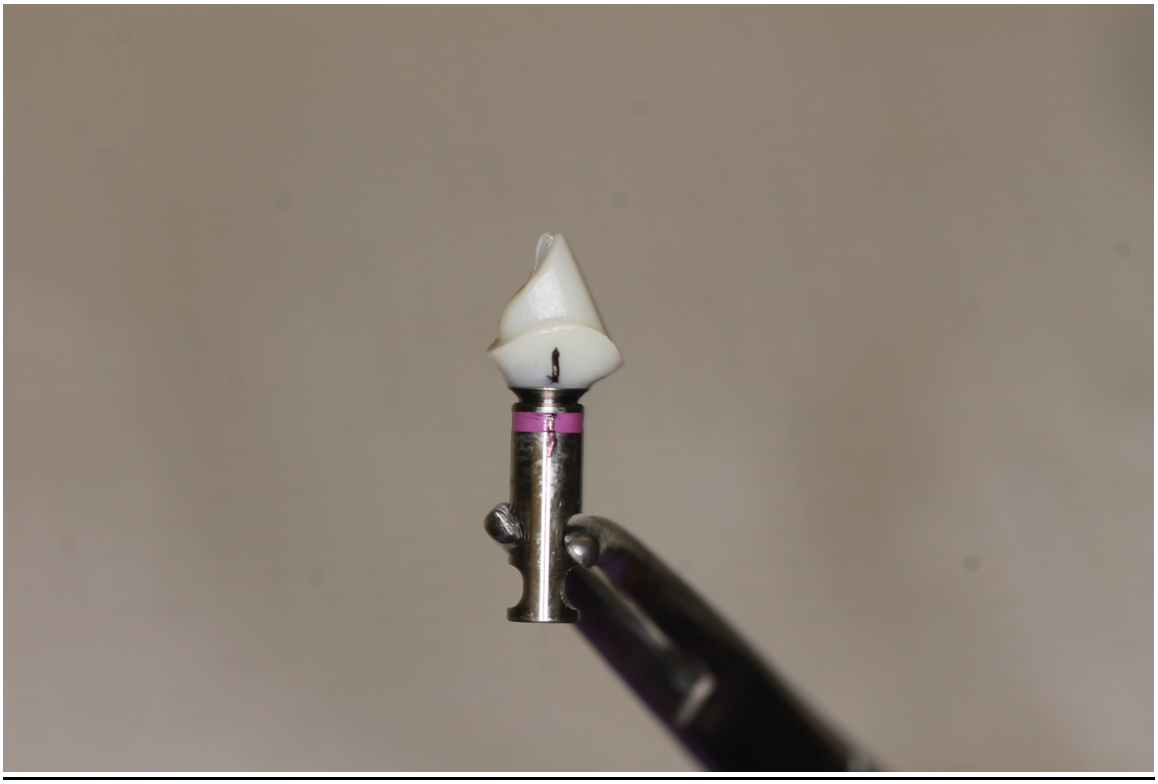

FIGURE 18.

The titanium-base and customized anatomic structures were cemented in such a way that the position markings were aligned.

FIGURE 19.

The combination of titanium-base and customized anatomic structures were autoclaved.

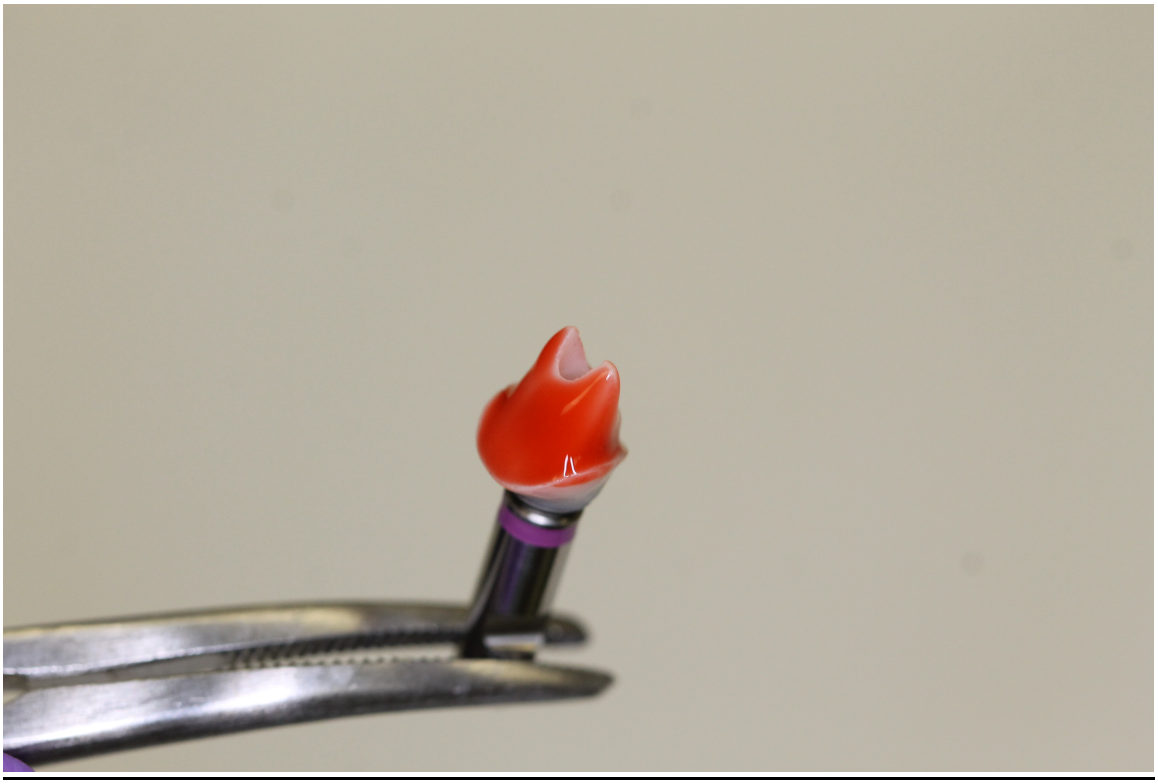

FIGURE 20.

The bonding interface of the customized anatomic structures was prepared 5% HF for 20 seconds.

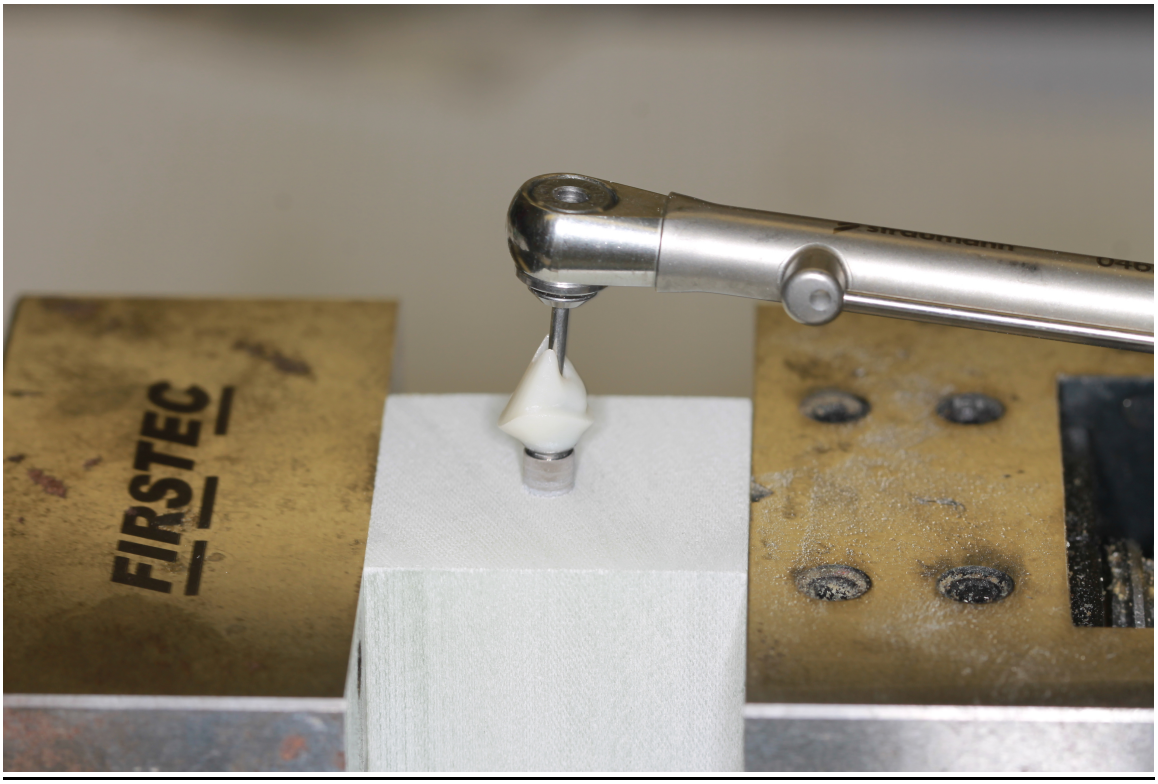

FIGURE 21.

The combination of titanium-base and customized anatomic structures were connected on dental implant embedded in specimen holder and torqued up to 35 Ncm using a manual torque wrench.

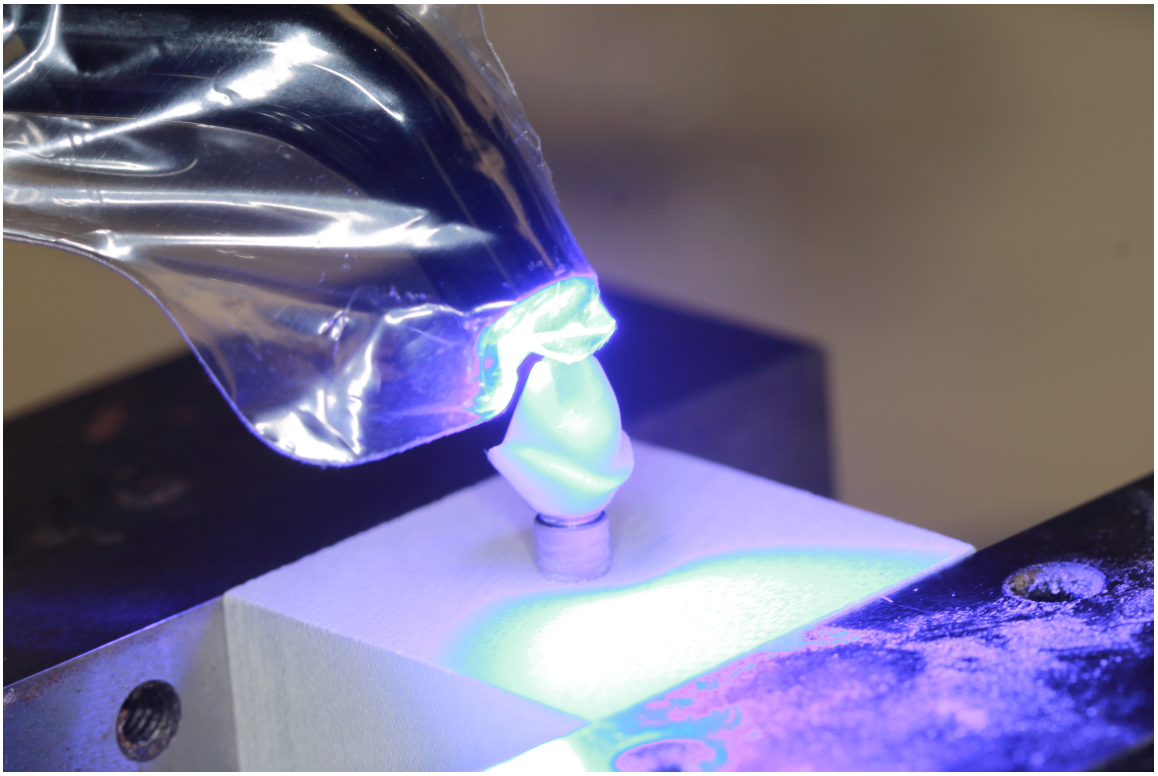

FIGURE 22.

The Telio CS inlay Universal was polymerized with a LED curing light.

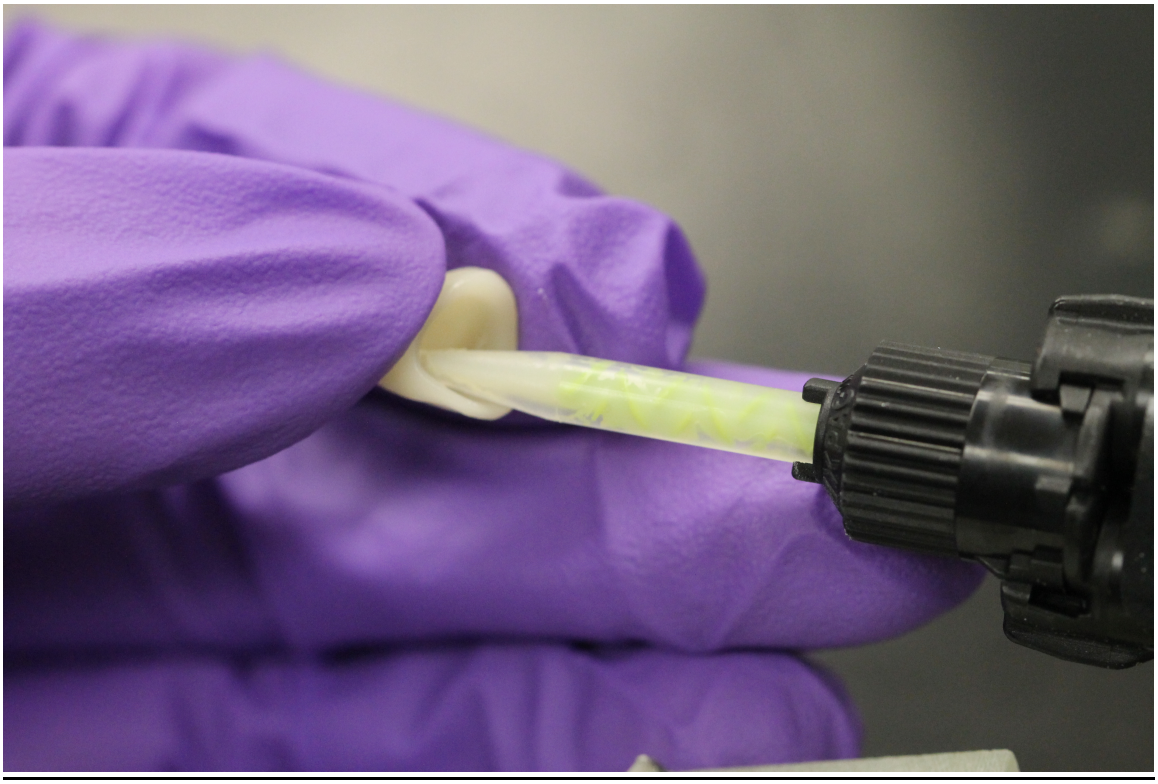

FIGURE 23.

All treated surface crowns were cemented to the customized anatomic structures with resin cement.

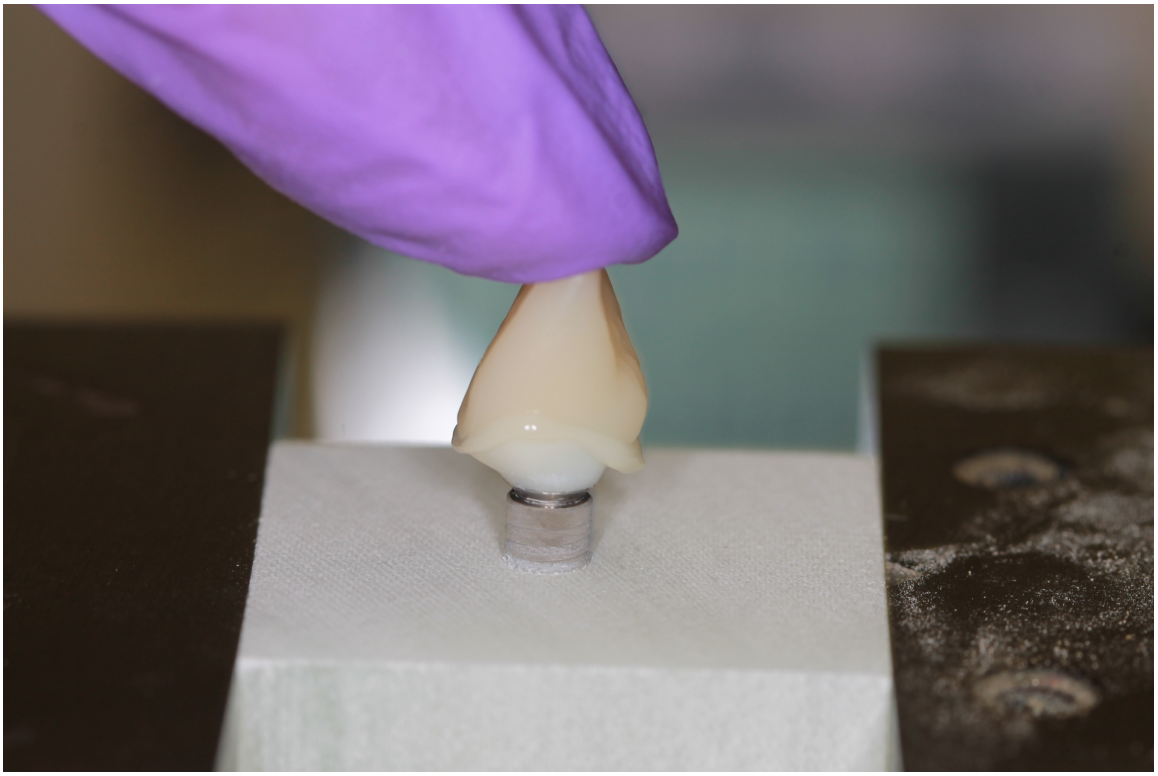

FIGURE 24.

The excess luting agent was removed with microbrush.

FIGURE 25.

The specimens were applied 300 grams of load.

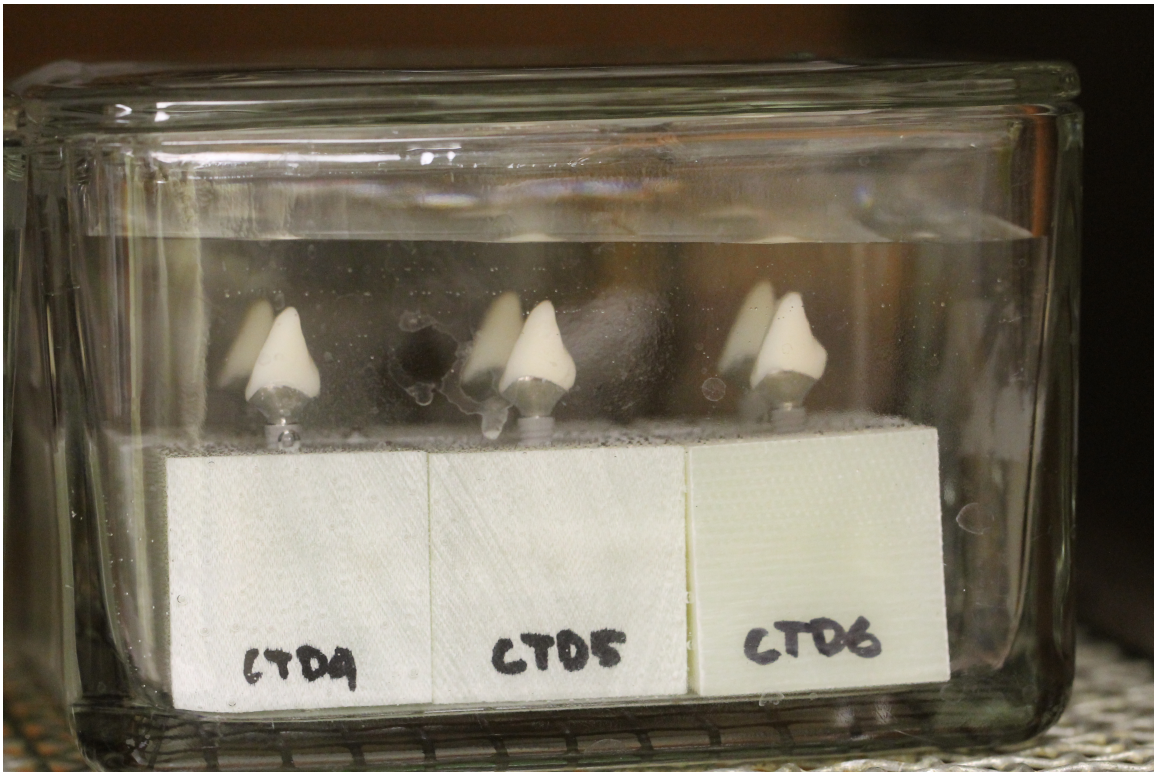

FIGURE 26.

All specimens were soaked under deionized water in the 37 °C incubator for 24 hours before testing.

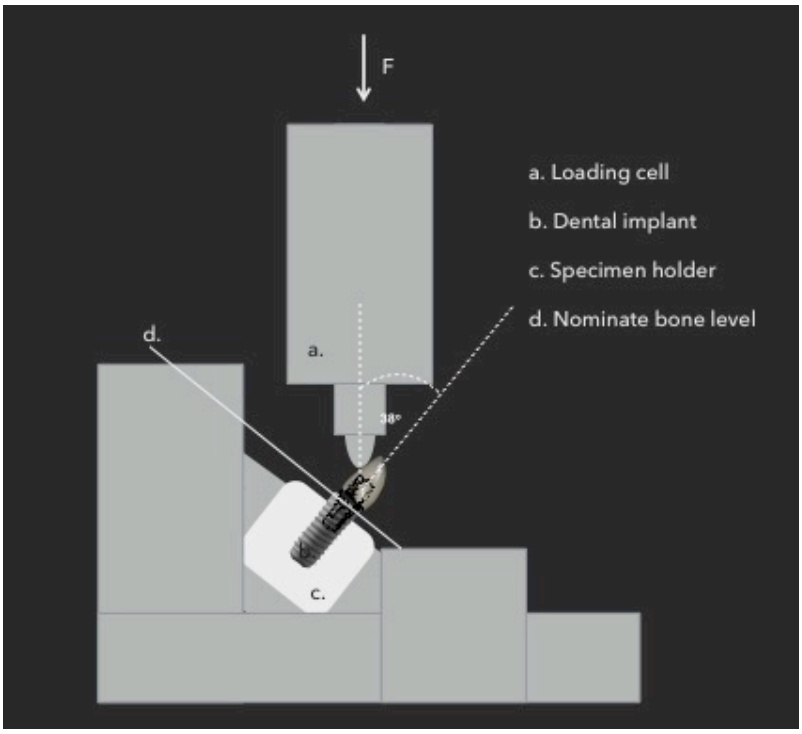

FIGURE 27.

Illustration of the testing setup in Instron E3000 machine

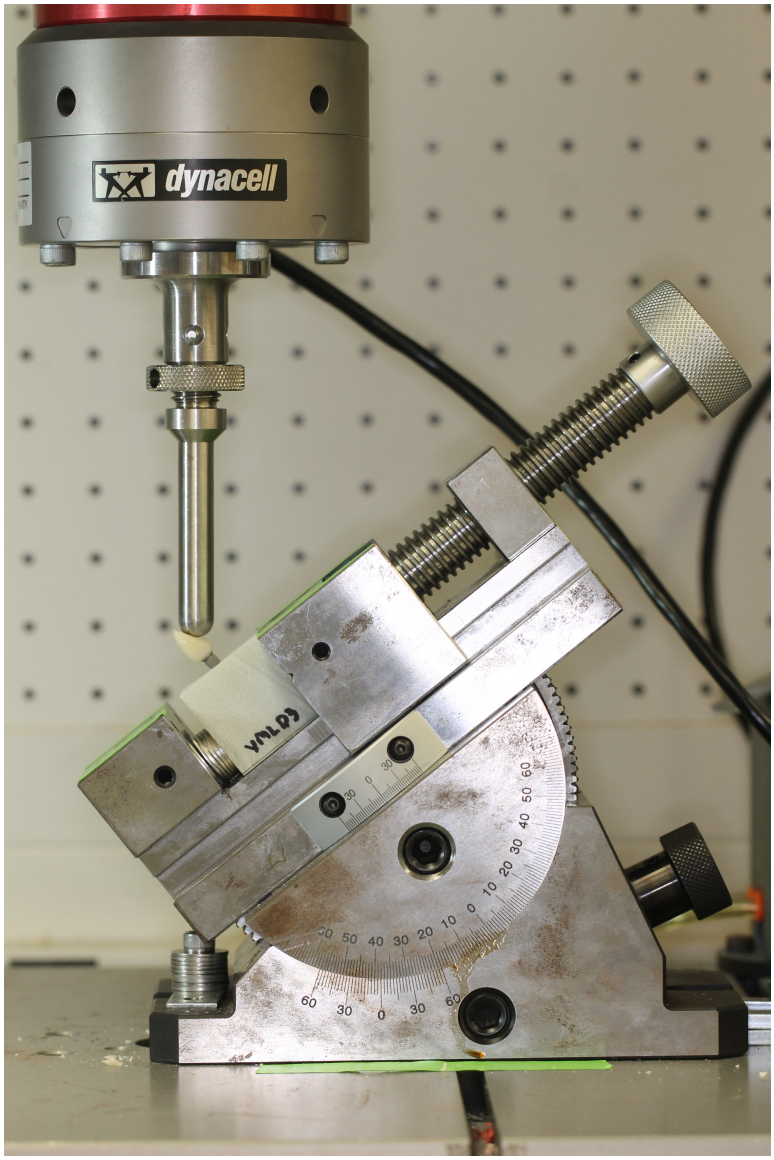

FIGURE 28.

All specimens were positioned at 38 ± 2 degrees to the long axis of the prosthesis.

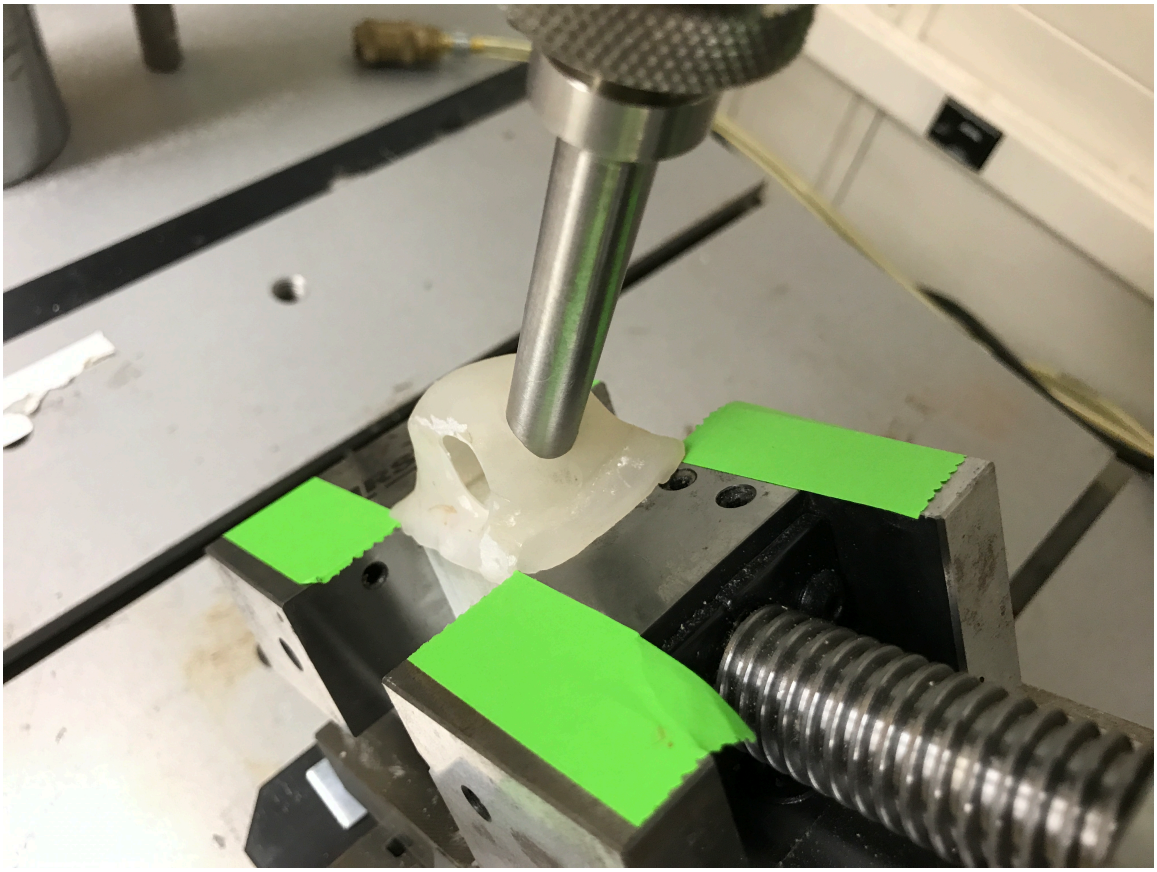

FIGURE 29.

A reposition device was utilized to locate the position of specimens.

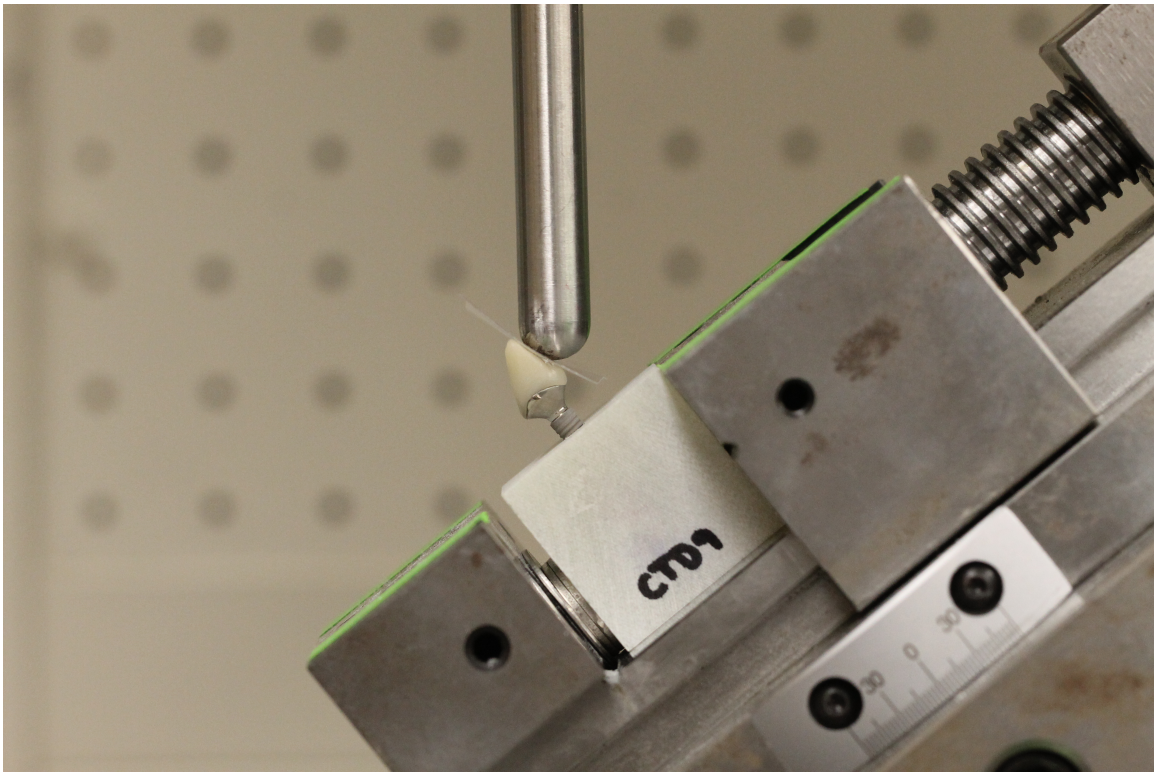

FIGURE 30.

Before fatigue loading for CTD specimen

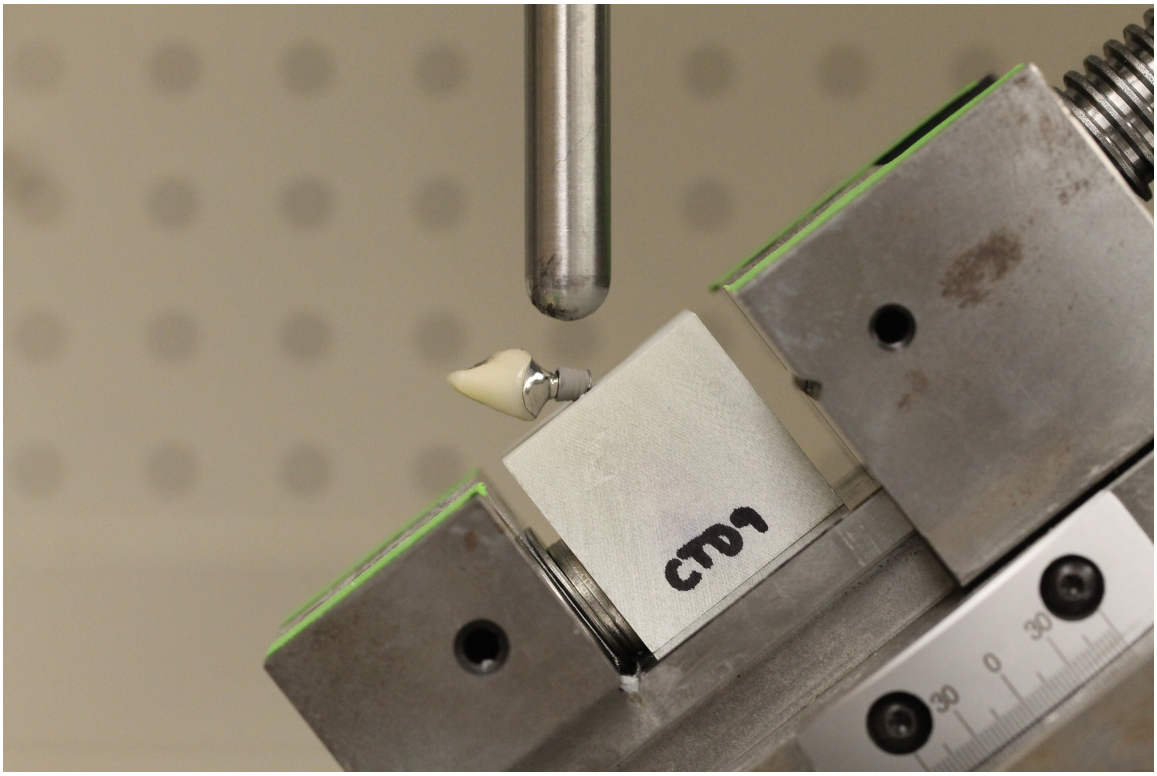

FIGURE 31.

After fatigue loading for CTD specimen presented implant and abutment screw fracture.

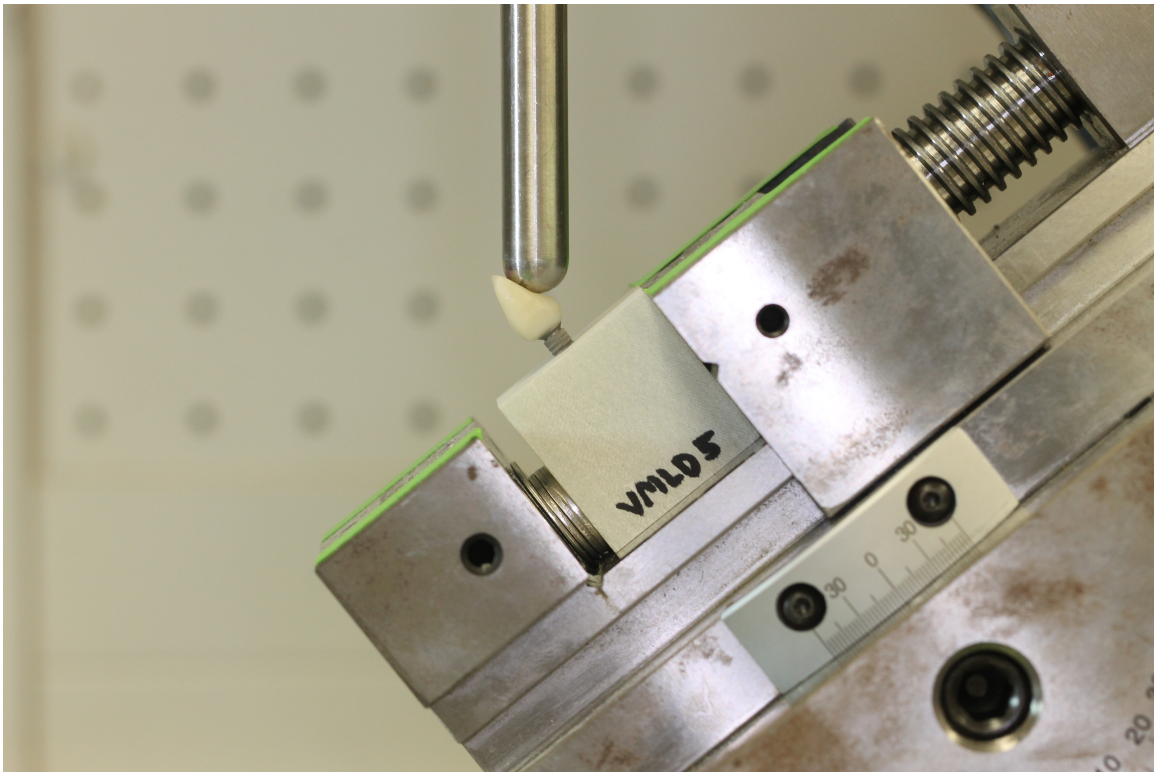

FIGURE 32.

Before fatigue loading for VMLD specimen

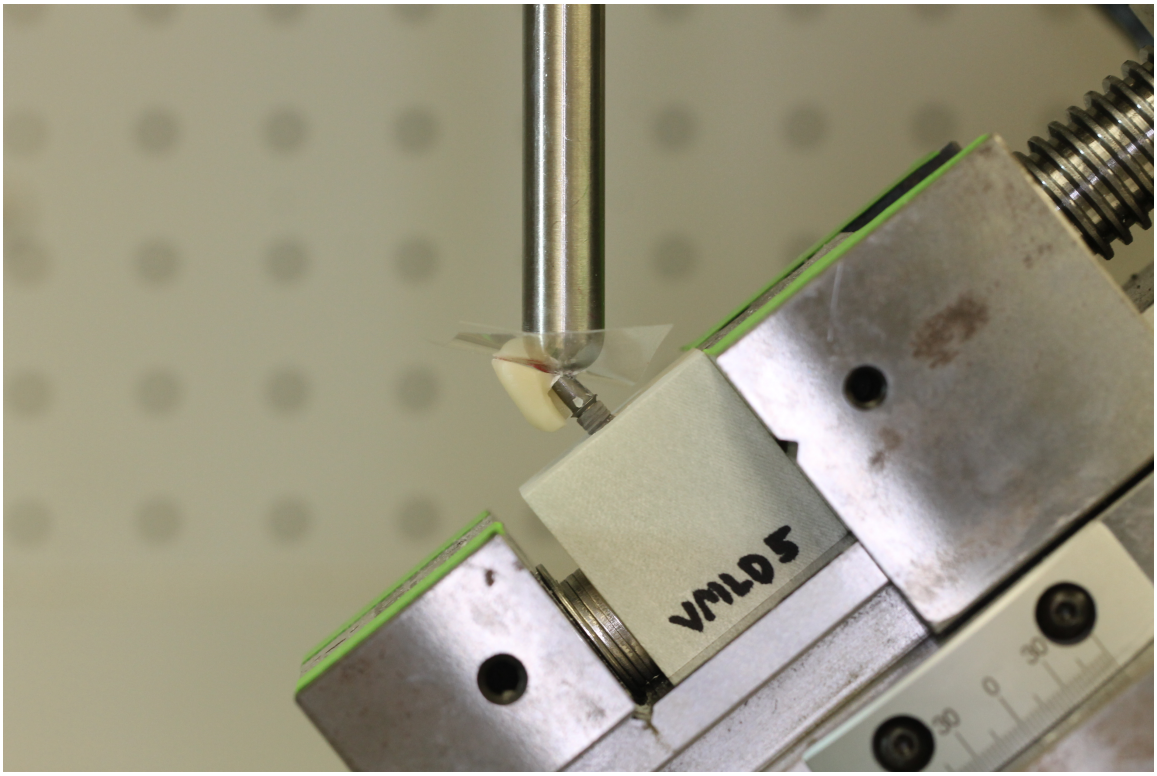

FIGURE 33.

After fatigue loading for VMLD specimen presented monolithic crown fracture.

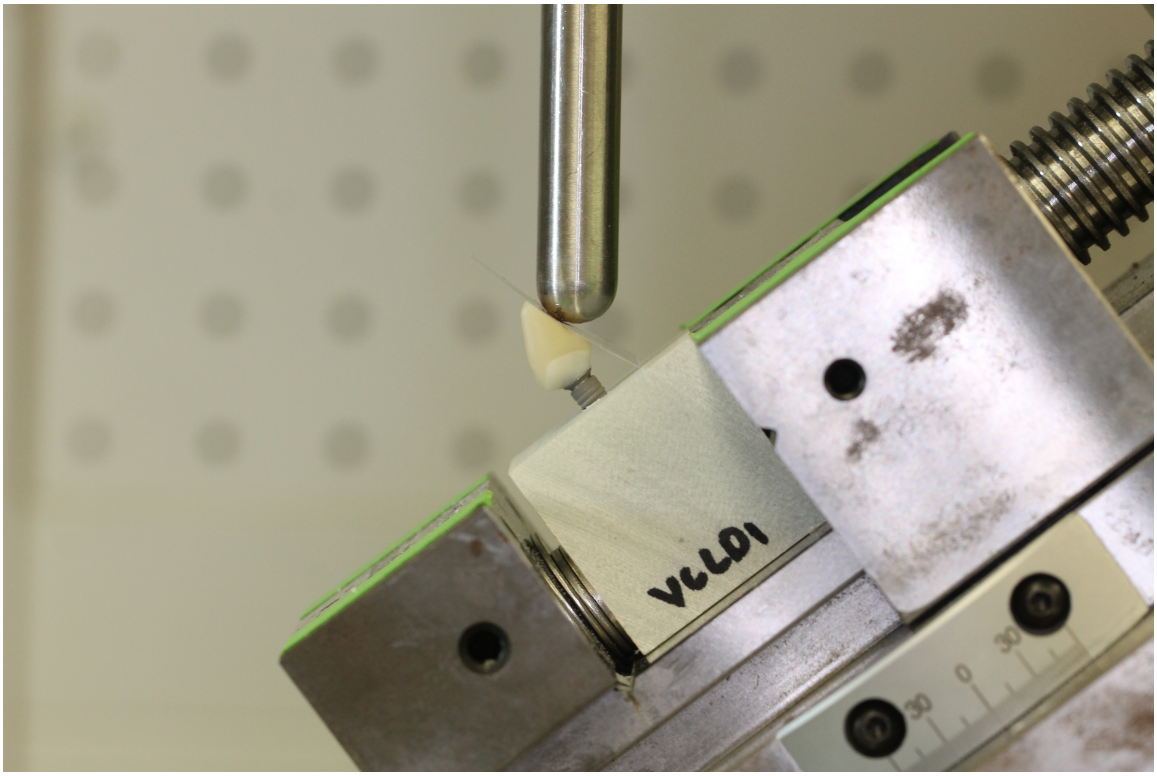

FIGURE 34.

Before fatigue loading for CTD specimen.

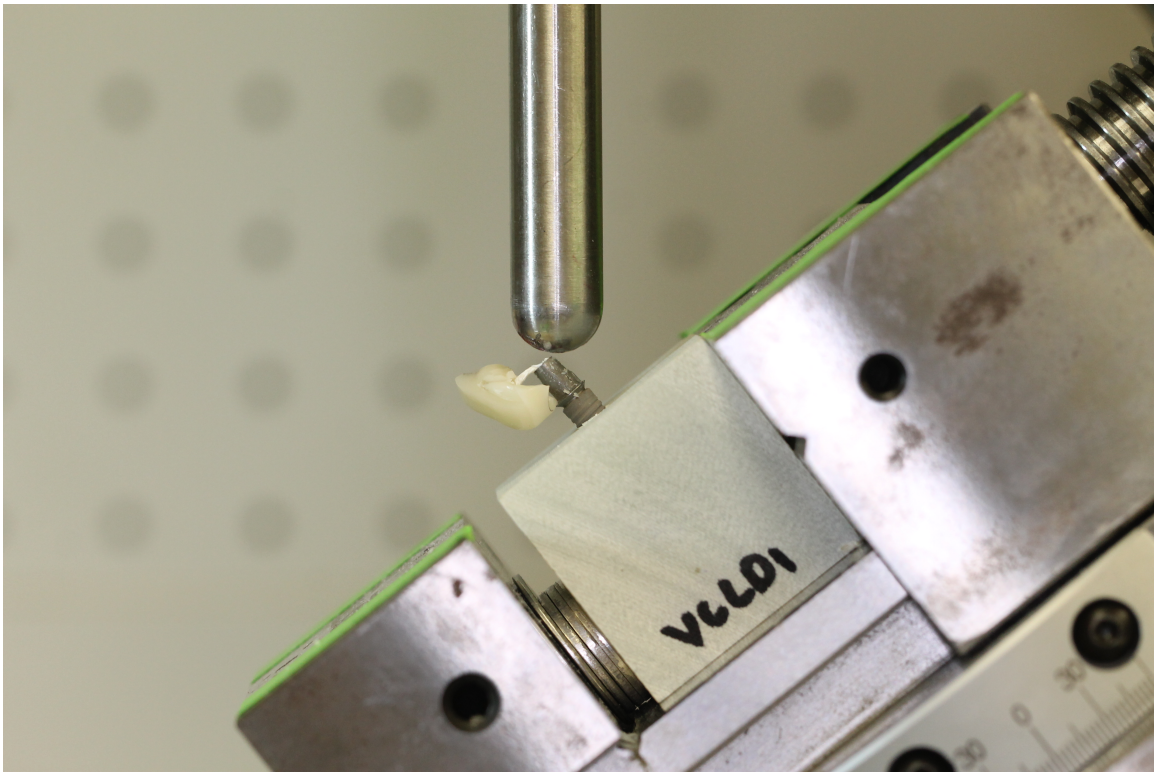

FIGURE 35.

After fatigue loading for VCLD specimen presented customized anatomical structure and crown fracture.

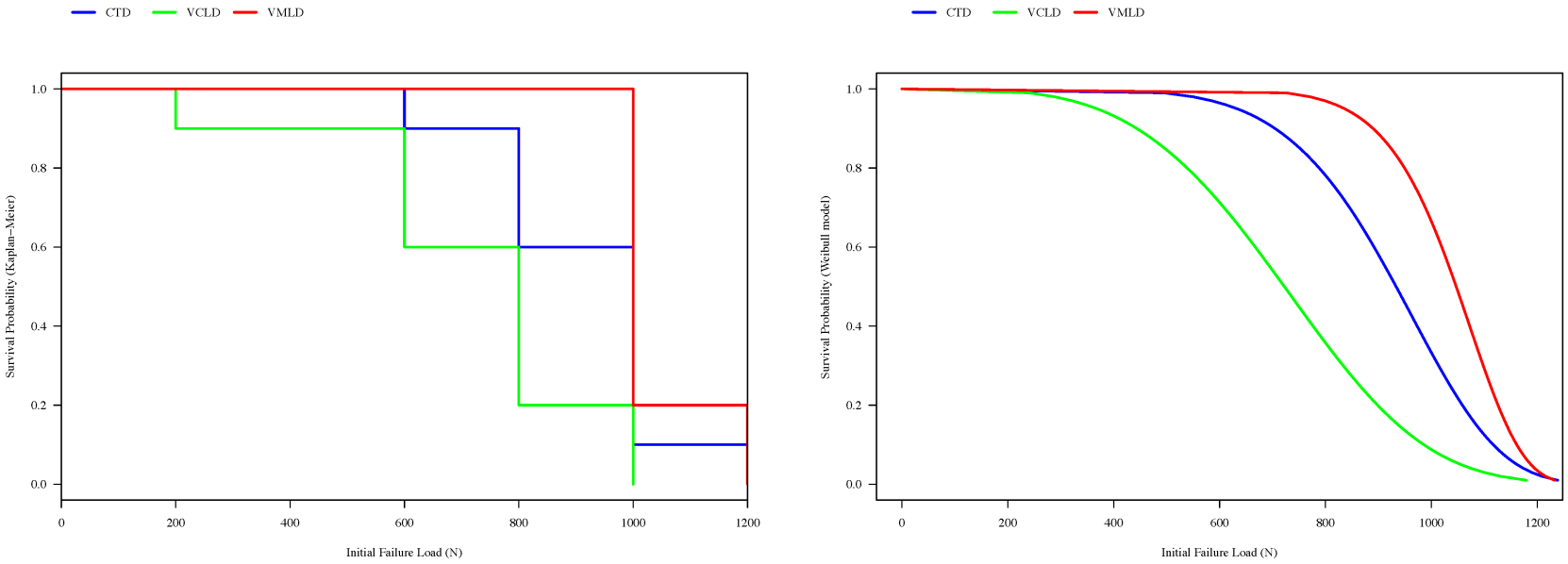

FIGURE 36.

Survival probability Kaplan−Meier and Weibull model of initial failure.

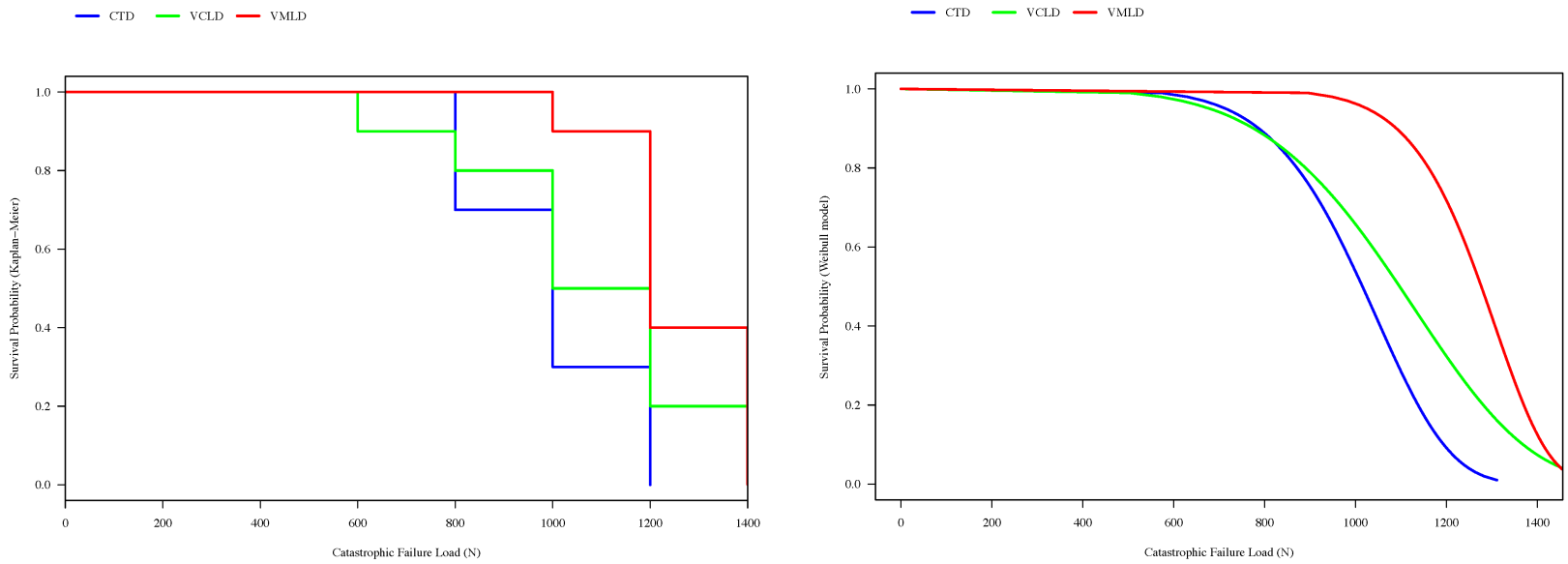

FIGURE 37.

Survival probability Kaplan−Meier and Weibull model of catastrophic failure.

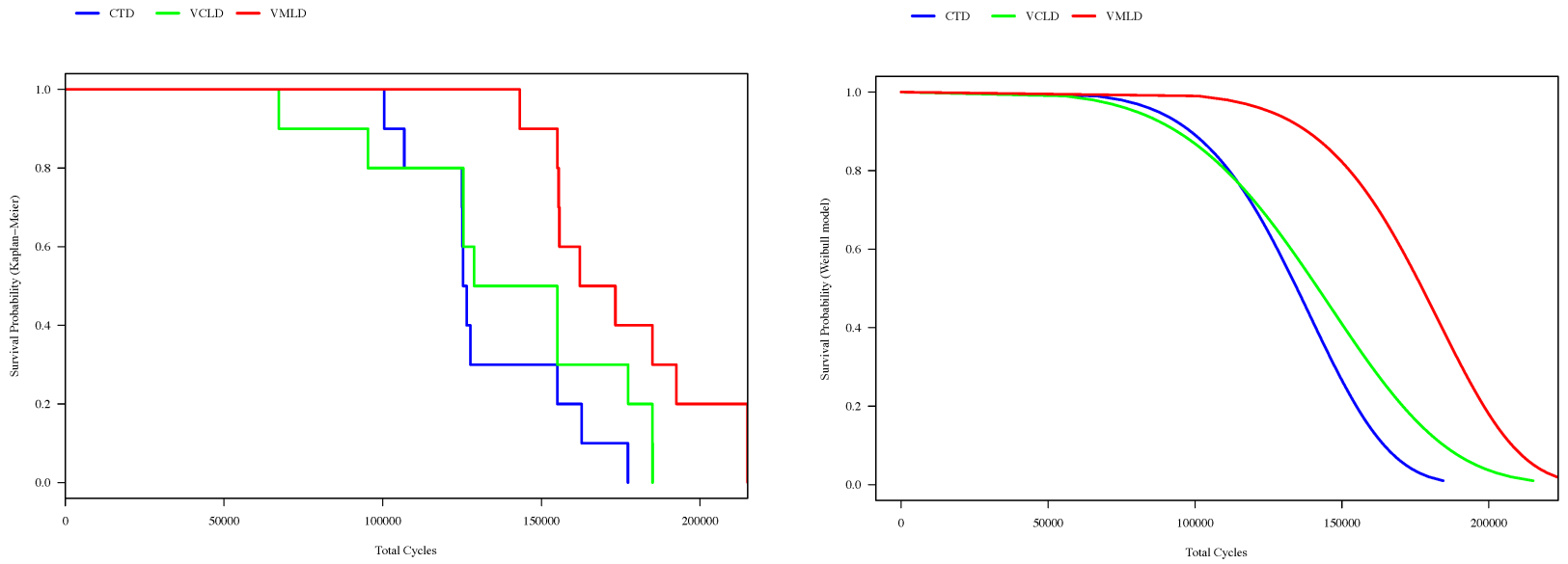

FIGURE 38.

Survival probability Kaplan−Meier and Weibull model of total cycles.

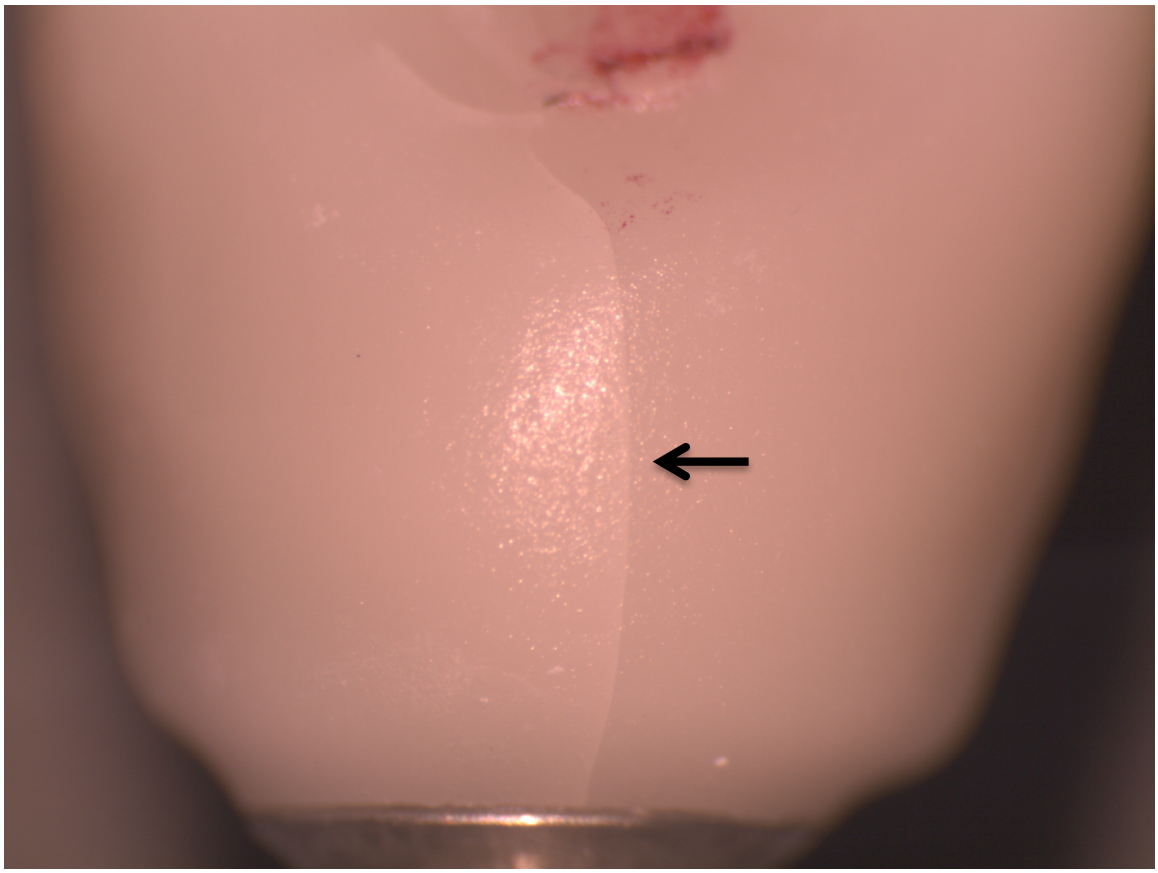

FIGURE 39.

One of VMLD specimen showed a crack line (black arrow) associated with screw channel on lingual aspect and titanium-base at 1000 N (2.5 × magnification)

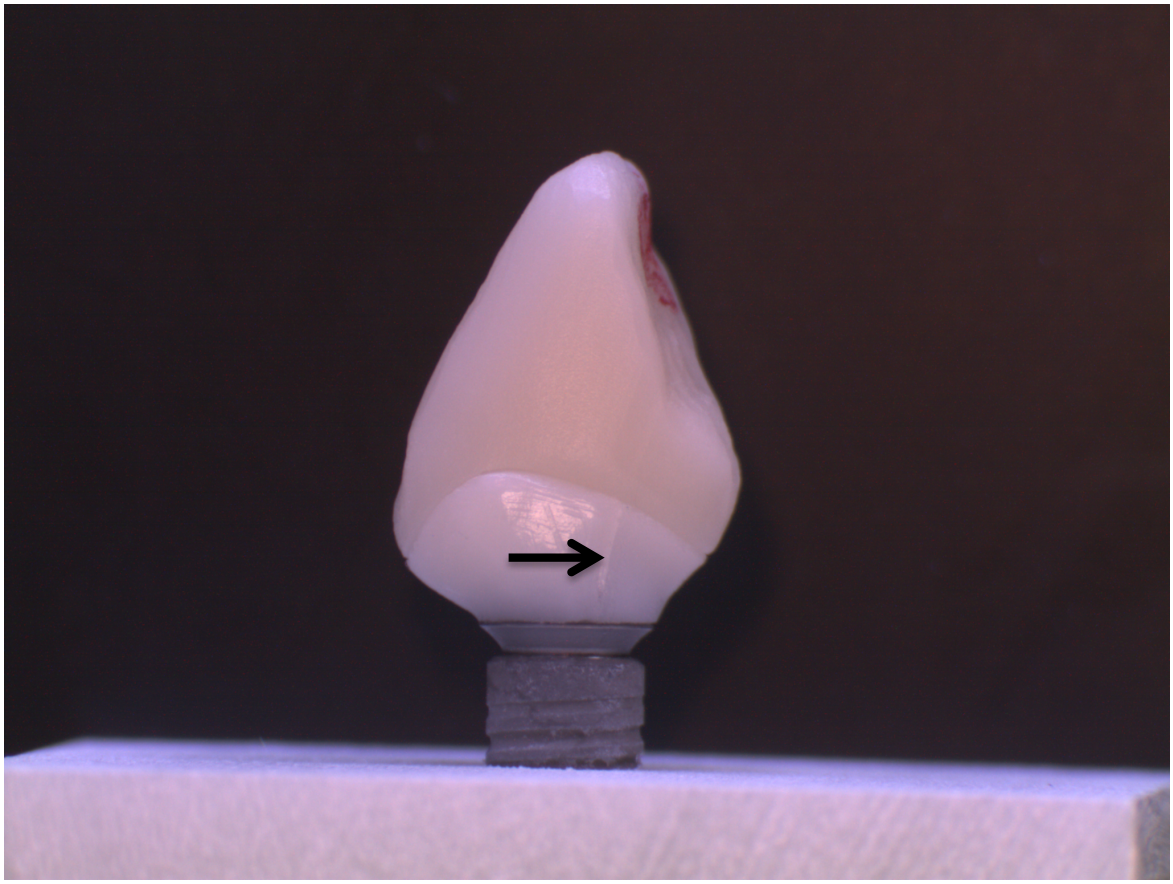

FIGURE 40.

One of VCLD specimen showed a crack line on lithium disilicate customizes anatomical structure at 800 N (black arrow) (0.8 × magnification).

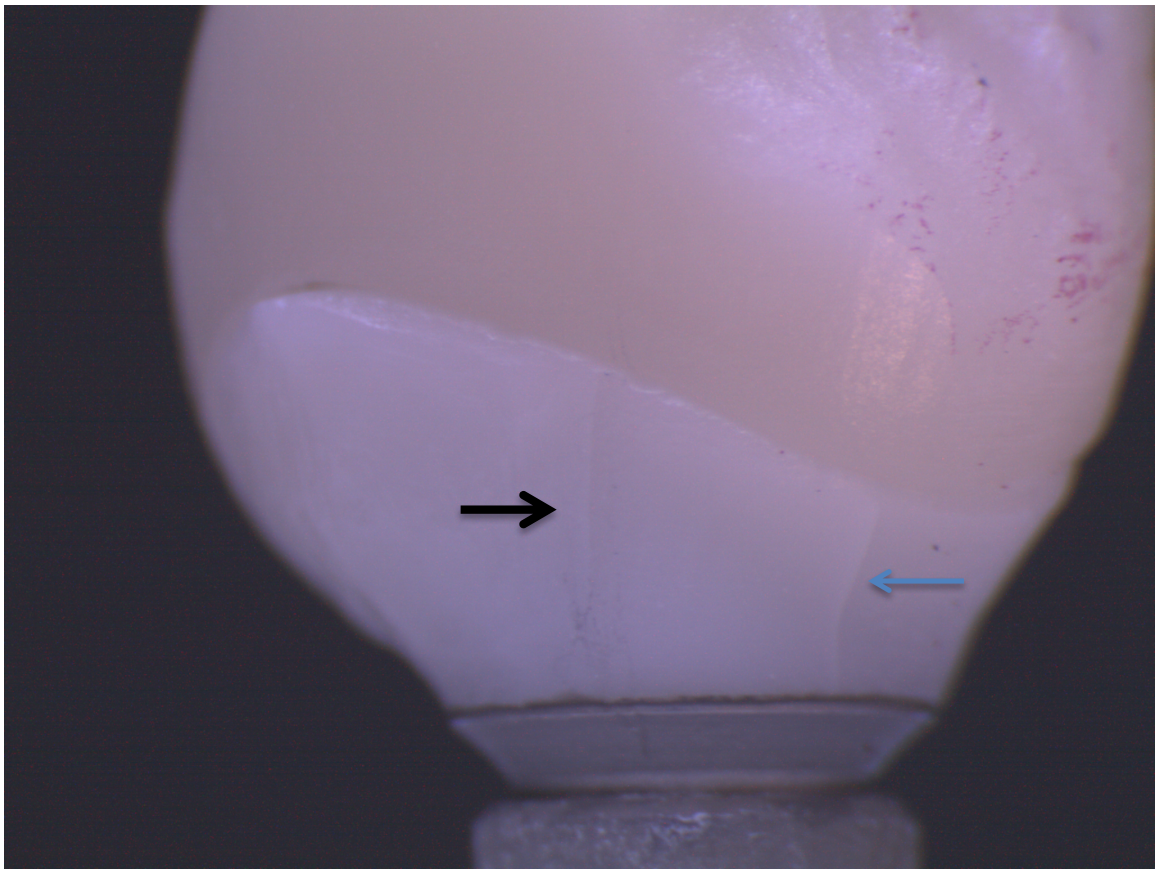

FIGURE 41.

One of VCLD specimen showed a crack line on lithium disilicate customizes anatomical structure at 800 N (black arrow) and 1000 N (blue arrow) (2.5 × magnification).

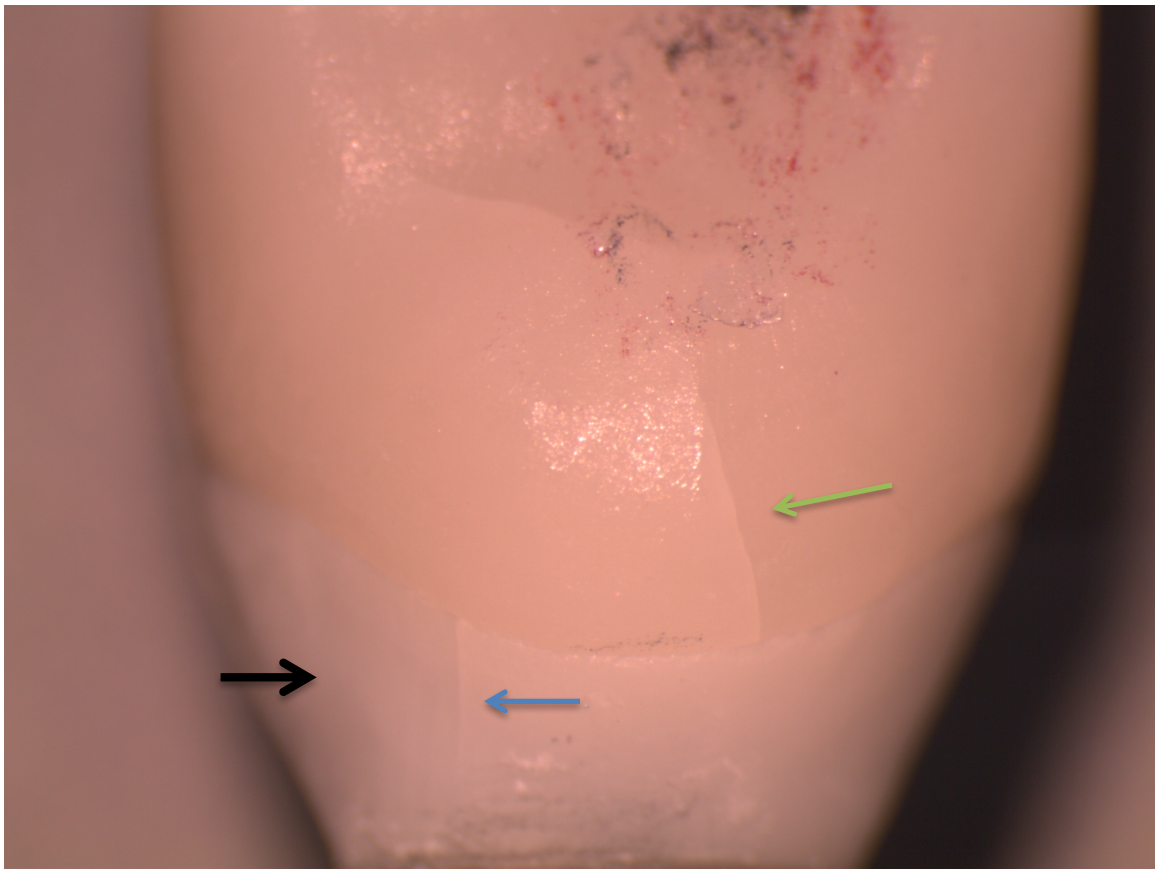

FIGURE 42.

One of VCLD specimen showed a crack line on lithium disilicate customizes anatomical structure at 800 N (black arrow), 1000 N (blue arrow), and 1200 N on crown (green arrow) (2.25 × magnification).

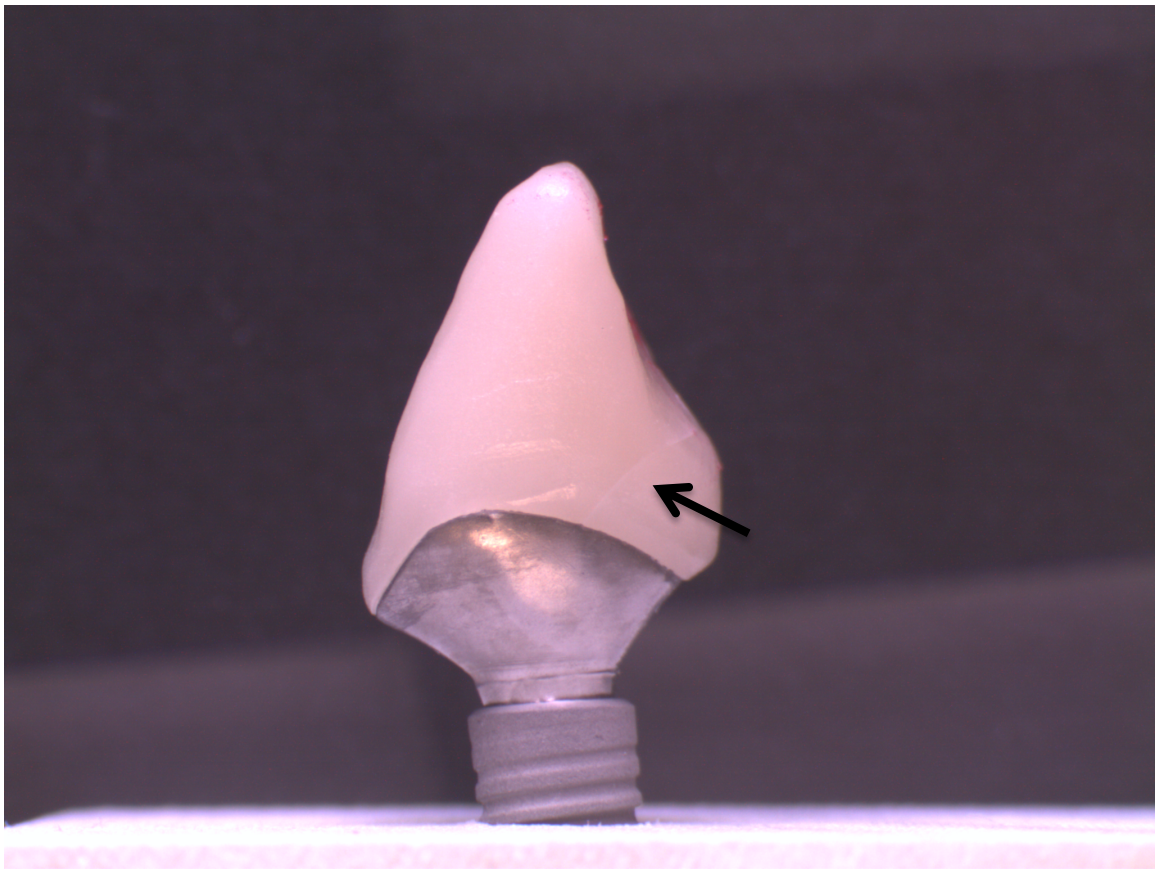

FIGURE 43.

One of CTD specimen showed a crack line on lithium disilicate crown at 800 N (black arrow) (0.8 × magnification).

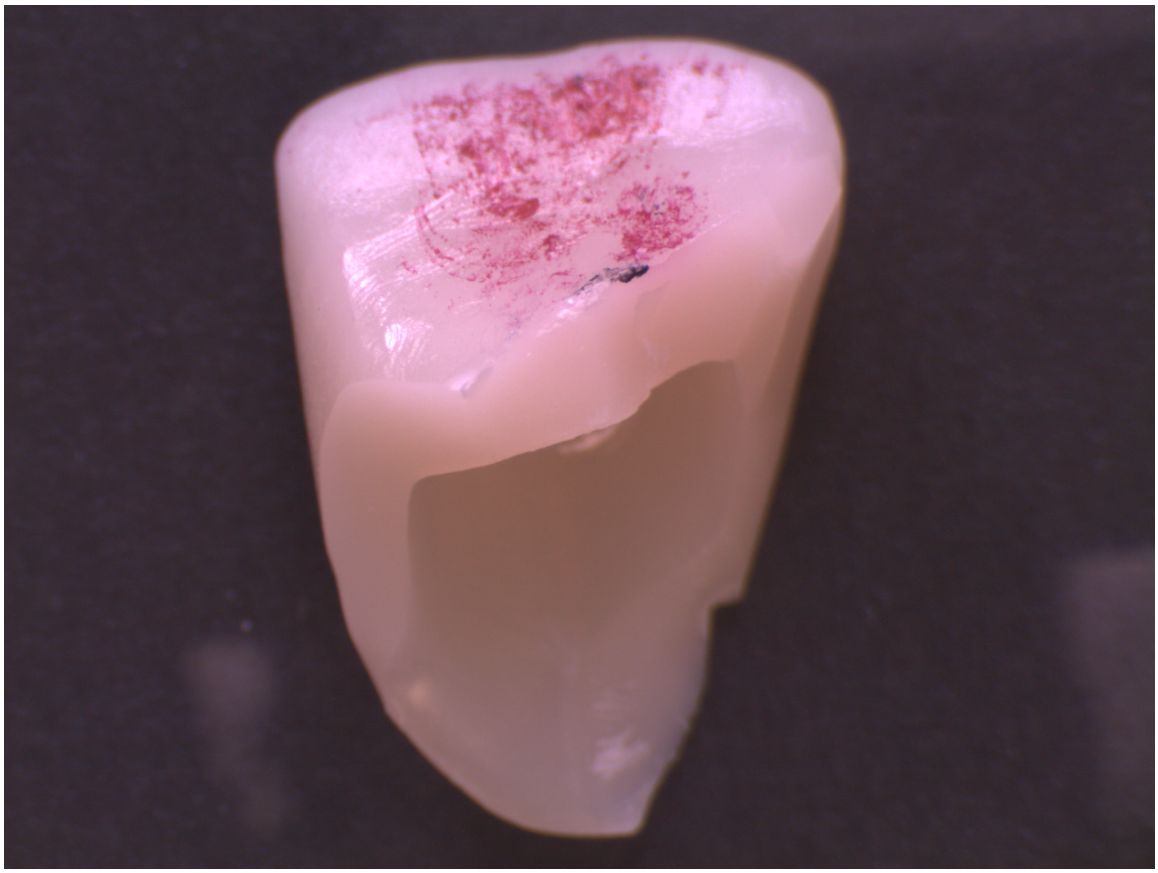

FIGURE 44.

One of CTD's lithium disilicate crown fractures (1.25 × magnification).

Description	Product Name	Manufacture	Lot / REF Number
Firing Pastes	Object Fix Putty	Ivoclar Vivadent, INC. Amherst, NY	W15018
Resin Cement	Multilink Implant (Transparent)		W05595
Silane	Monobond Plus		W02294
Hydrofluoric Acid Etching Gel (HF)	IPS ceramic etching		W04959
Glycerine gel	Liquid Strip Refill		V51366
Implant Channel Sealing Material	Telio Inlay CS		W07643
Resin Composite	Tetric EvoCeram A2		W10431
Silicone Light Body	Virtual Ref Extra Light Body Fast Set		VL2308
Finisher Bur	OptraFine F Flame Refill		VL0798
Polishing Bur	OptraFine P Flame Refill		VL0870
Nylon Brush	OptraFine HP Nylon Brush Refill		VL0725
Polishing Paste	OptraFine HP Polishing Paste Refill		WL0715
Monolithic Crown	E.max Monolithic Crown LT A1		S4357
E.max crown	E.max Crown LT A2		REF 634006
E.max Custom Anatomical Structure	E.max Custom Abutment MO1		REF 634004
Dental Implant	Bone Level Implant 4.1 mm RC	Straumann, LLC Boston, MA	MG236 NH934
Titanium-based	RC Straumann Variobase for CEREC		NH471 NG663
Implant Analog	RC Implant Analog		MR035
Titanium Custom Abutment	Straumann CARES Titanium Custom Abutment	Straumann Scan and Shape Arlington, TX	REF 027.4620
Straumann e.max Crown	Straumann CARES e.max Crown		REF 010.5001
Diamond Disc	MED Disc H DBL 1P	Brasseler USA Savannah, GA	K95PD
Epoxy Resin-Glass Fiber Composite Specimen Holder	NEMA Grade G-10	Piedmont Plastics	138390

TABLE I.

Materials used in the study.

Group	Number of Specimens	Base of Abutment	Customized Anatomic Structure	Crown
CTD	10	Straumann® CARES® Titanium custom abutment		Lithium disilicate
VMLD	10	Variobase® for CEREC® Titanium-base	Monolithic lithium disilicate	
VCLD	10	Variobase® for CEREC® Titanium-base	Lithium disilicate	Lithium disilicate
Total	30			

TABLE II.

Different abutment and crown options

Program	Stand-by temp B [°C]	Closing time S [min]	Heating rate t_1 [°C/min]	Firing temp T_1 [°C]	Holding time H_1 [min]	Heating rate t2 [°C/min]	Firing temp T_2 [°C]	Holding time H_2 [min]	Vacuum1 $1_1/1_2$ [°C]	Vacuum2 $2_1/2_2$ [°C]	Long-term cooling L [°C]	Cooling rate t_l [°C/min]
1	403	06:00	90	820	00:10	30	840	07:00	550/820	820/840	700	0
7	403	06:00	60	770	00:10	30	850	10:00	550/770	770/850	700	0

TABLE III.

Crystallization and firing parameters for programat CS furnaces

Group	Initial Failure Load (N)				Catastrophic Failure Load (N)				Number of Cycles			
	Mean	SE	95% Confidence Interval		Mean	SE	95% Confidence Interval		Mean	SE	95% Confidence Interval	
			Lower Bound	Upper Bound			Lower Bound	Upper Bound			Lower Bound	Upper Bound
CTD	920[b]	53	799	1041	1000[b]	52	883	1117	133185[b]	7694	115780	150590
VMLD	1040[b]	27	980	1100	1260[a]	43	1163	1357	175231[a]	8126	156847	193614
VCLD	720[a]	74	552	888	1080[b]	80	899	1261	139965[b]	12352	112022	167908

[a] The same lower case letters denote no significant statistical difference.

TABLE IV.

The initial and catastrophic failure loads and number of cycles.

Group	Initial Failure		Catastrophic Failure		Number of Cycles	
	Weibull Characteristic Strength	Weibull Modulus	Weibull Characteristic Strength	Weibull Modulus	Weibull Characteristic Strength	Weibull Modulus
CTD	986	6.7	1067	7.4	143163	6.0
VMLD	1081	11.6	1317	11.9	186199	7.6
VCLD	794	3.9	1174	5.4	153795	4.6

TABLE V.

The Weibull characteristic strength and modulus.

Group	Implant	Titanium Custom Abutment	Titanium-Base	Customized Anatomical Structure	Abutment Screw	Crown	Monolithic Crown
CTD	4	0	N/A	N/A	4	7	N/A
VMLD	2	N/A	0	N/A	2	N/A	6
VCLD	3	N/A	0	7	3	8	N/A
% of Failure	30%	0%	0%	70%	30%	75%	60%

TABLE VI.

Mode of failure at catastrophic failure load (n=10/sample)
N/A means no specific component on specific restorative designs.

DISCUSSION

The present study aimed to investigate the fatigue limit of three different designs of lithium disilicate anterior tooth restoration cemented on titanium-base. After the data collection, the null hypothesis was rejected, since the fatigue experiment showed that titanium-base cemented with monolithic lithium disilicate crown (VMLD) survived a higher number of cycles and resisted to higher failure load comparing to the custom titanium abutment (CTD) and a lithium disilicate customized anatomical structure cemented crown (VCLD).

Several studies have tried to provide information regarding the longevity of titanium-base for anterior tooth restoration. A clinical case report evaluated the use of the chairside titanium-base cemented with both cement- or screw-retained ceramic restorations. The authors concluded that both techniques can prevent the consequence of excess cement around the implant, create the better dentogingival esthetic, and deliver the final restoration in single appointment.[11] A different author published two studies[10, 39] using the proprietary titanium-base. The first study reported that a proprietary titanium-base and zirconia abutment connected with monolithic lithium disilicate material had the highest mechanical stiffness and failure load comparing to nonproprietary titanium-base and zirconia abutments.[10] Whereas the second experiment presented the similar results for titanium-base group cemented with Resin Nano Ceramic (RNC) material.[39] Although both studies[10, 39] had followed ISO 14801[33] standard by fabricating the restoration as a dome shape cemented on abutment, this study tried to simulate a clinical scenario by incorporating chairside proprietary titanium-base and represented the anterior tooth anatomy in our methodology.

The result of this study showed significant statistical difference of VMLD catastrophic failure loads and total cycles. The data presented that all the initial failures of the VMLD group were associated with the location of the screw channel. This finding suggested that the location of the screw channel might influence the mode of failure of VMLD design base on the worst-case scenario of implant marginal bone loss. In contrast, findings from previous studies,[12, 24] that embedded the implant at the normal bone level reported a permanent plastic deformation at the screw and internal connection of titanium-base without ceramic displacement or fracture.[12]

After observing initial failure behavior, it was observed that the weakest component for the VCLD group is a lithium disilicate customized anatomical structure. Increasing the thickness of the lithium disilicate customized anatomical structure; the authors believed that it might increase the fatigue limit of the VCLD design. However, the thickness of the emergence profile is limited to the diameter of the titanium-base and implant.

The survival probability Kaplan−Meier and Weibull diagram showed that the VCLD initial failure load was relatively the lowest in all three groups. This failure behavior from the VCLD group could be explained by the presence of resin cement between the ceramic structures. The VCLD specimens tended to survive with fatigue loading in a longer interval than the VMLD and CTD groups before catastrophic failure occurred. Previous studies had reported that bilayer ceramic cementation can limit or arrest subcritical crack growth in regions near the cement layer, which is consistent with the present study finding.[40, 41]

A 70% failure of the CTD group was a fracture of lithium disilicate crown with some custom titanium abutment deformation, which can be explained by the ceramics brittle characteristic. However, the initial failure load of the CTD group was still significantly higher than the VCLD group. This could be assuming that custom titanium abutment cemented with lithium disilicate crown is impregnable to sustain a fatigue loading. The author also found a 30% failure mode was the fracture at a tensile side of abutment screws and implants all across three groups. This finding is in agreement with a recent study[34], which reported the failures in the similar locations when testing tissue level implant in worst-case scenario. This can imply that fracturing of abutment screws and implants are not related to the design of restorations or choice of abutments.

It appeared that lithium disilicate abutments and crowns connected to titanium-base, that underwent stepwise fatigue loading, had a similar fatigue resistance to custom titanium abutments cemented lithium disilicate abutment crowns in regards to restoring the anterior tooth restoration. In summary, all three groups could bear a greater load than normal chewing forces[22], which is consistent with other studies[12, 24]. The limitation of this study is the BullHill 2.0 software, which cannot automatically record the initial failure loads. The initial failure was visually observed at the end of each cycle under the light microscope. In addition, the axial loading without sliding load from the specimens had to be meticulously monitor throughout the experiment. Further study is needed to investigate behavior of the reduced diameter implant and abutment restoring with lithium disilicate and titanium-base.

SUMMARY AND CONCLUSIONS

Due to the limitation of this in vitro study, the following conclusions were drawn:

VMLD performs the best fatigue resistance when compared with the two other groups.

REFERENCES

1. Simonis P, Dufour T, Tenenbaum H. Long-term implant survival and success: a 10-16-year follow-up of non-submerged dental implants. Clin Oral Implants Res 2010;21(7):772-7.
2. den Hartog L, Slater JJ, Vissink A, Meijer HJ, Raghoebar GM. Treatment outcome of immediate, early and conventional single-tooth implants in the aesthetic zone: a systematic review to survival, bone level, soft-tissue, aesthetics and patient satisfaction. J Clin Periodontol 2008;35(12):1073-86.
3. Lee M-C, Wright RF. The SAC Classification in Implant Dentistry. Journal of Prosthodontics 2010;19(4):335-36.
4. Jung RE, Sailer I, Hammerle CH, Attin T, Schmidlin P. In vitro color changes of soft tissues caused by restorative materials. Int J Periodontics Restorative Dent 2007;27(3):251-7.
5. Adell R, Lekholm U, Rockler B, Branemark PI. A 15-year study of osseointegrated implants in the treatment of the edentulous jaw. Int J Oral Surg 1981;10(6):387-416.
6. Branemark PI. Osseointegration and its experimental background. J Prosthet Dent 1983;50(3):399-410.
7. Sailer I, Zembic A, Jung RE, Hammerle CH, Mattiola A. Single-tooth implant reconstructions: esthetic factors influencing the decision between titanium and zirconia abutments in anterior regions. Eur J Esthet Dent 2007;2(3):296-310.
8. Wadhwani C, Rapoport D, La Rosa S, Hess T, Kretschmar S. Radiographic detection and characteristic patterns of residual excess cement associated with cement-retained implant restorations: A clinical report. The Journal of Prosthetic Dentistry 2012;107(3):151-57.
9. Marchack CB. A custom titanium abutment for the anterior single-tooth implant. J Prosthet Dent 1996;76(3):288-91.
10. Joda T, Burki A, Bethge S, Bragger U, Zysset P. Stiffness, Strength, and Failure Modes of Implant-Supported Monolithic Lithium Disilicate Crowns: Influence of Titanium and Zirconia Abutments. Int J Oral Maxillofac Implants 2015;30(6):1272-9.
11. Kurbad A, Kurbad S. CAD/CAM-based implant abutments. Int J Comput Dent 2013;16(2):125-41.
12. Elsayed A, Wille S, Al-Akhali M, Kern M. Effect of fatigue loading on the fracture strength and failure mode of lithium disilicate and zirconia implant abutments. Clin Oral Implants Res 2017.
13. Lin WS, Harris BT, Zandinejad A, Martin WC, Morton D. Use of prefabricated titanium abutments and customized anatomic lithium disilicate structures for cement-retained implant restorations in the esthetic zone. J Prosthet Dent 2014;111(3):181-5.
14. Stimmelmayr M, Sagerer S, Erdelt K, Beuer F. In vitro fatigue and fracture strength testing of one-piece zirconia implant abutments and zirconia implant abutments connected to titanium cores. Int J Oral Maxillofac Implants 2013;28(2):488-93.

15. Foong JK, Judge RB, Palamara JE, Swain MV. Fracture resistance of titanium and zirconia abutments: an in vitro study. J Prosthet Dent 2013;109(5):304-12.
16. Stimmelmayr M, Edelhoff D, Guth JF, et al. Wear at the titanium-titanium and the titanium-zirconia implant-abutment interface: a comparative in vitro study. Dent Mater 2012;28(12):1215-20.
17. Yilmaz B, Salaita LG, Seidt JD, McGlumphy EA, Clelland NL. Load to failure of different zirconia abutments for an internal hexagon implant. J Prosthet Dent 2015.
18. Att W, Yajima ND, Wolkewitz M, Witkowski S, Strub JR. Influence of preparation and wall thickness on the resistance to fracture of zirconia implant abutments. Clin Implant Dent Relat Res 2012;14 Suppl 1:e196-203.
19. Tan K, Pjetursson BE, Lang NP, Chan ES. A systematic review of the survival and complication rates of fixed partial dentures (FPDs) after an observation period of at least 5 years. Clin Oral Implants Res 2004;15(6):654-66.
20. Jung RE, Pjetursson BE, Glauser R, et al. A systematic review of the 5-year survival and complication rates of implant-supported single crowns. Clin Oral Implants Res 2008;19(2):119-30.
21. Gibbs CH, Mahan PE, Lundeen HC, et al. Occlusal forces during chewing and swallowing as measured by sound transmission. J Prosthet Dent 1981;46(4):443-9.
22. Gibbs CH, Mahan PE, Mauderli A, Lundeen HC, Walsh EK. Limits of human bite strength. J Prosthet Dent 1986;56(2):226-9.
23. Haraldson T, Carlsson GE, Ingervall B. Functional state, bite force and postural muscle activity in patients with osseointegrated oral implant bridges. Acta Odontol Scand 1979;37(4):195-206.
24. Elsayed A, Wille S, Al-Akhali M, Kern M. Comparison of fracture strength and failure mode of different ceramic implant abutments. J Prosthet Dent 2017;117(4):499-506.
25. Wolf D, Bindl A, Schmidlin PR, Luthy H, Mormann WH. Strength of CAD/CAM-generated esthetic ceramic molar implant crowns. Int J Oral Maxillofac Implants 2008;23(4):609-17.
26. Belser UC, Grutter L, Vailati F, et al. Outcome evaluation of early placed maxillary anterior single-tooth implants using objective esthetic criteria: a cross-sectional, retrospective study in 45 patients with a 2- to 4-year follow-up using pink and white esthetic scores. J Periodontol 2009;80(1):140-51.
27. Furhauser R, Florescu D, Benesch T, et al. Evaluation of soft tissue around single-tooth implant crowns: the pink esthetic score. Clin Oral Implants Res 2005;16(6):639-44.
28. Zembic A, Bosch A, Jung RE, Hammerle CH, Sailer I. Five-year results of a randomized controlled clinical trial comparing zirconia and titanium abutments supporting single-implant crowns in canine and posterior regions. Clin Oral Implants Res 2013;24(4):384-90.
29. Sailer I, Zembic A, Jung RE, et al. Randomized controlled clinical trial of customized zirconia and titanium implant abutments for canine and

posterior single-tooth implant reconstructions: preliminary results at 1 year of function. Clin Oral Implants Res 2009;20(3):219-25.
30. Zembic A, Sailer I, Jung RE, Hammerle CH. Randomized-controlled clinical trial of customized zirconia and titanium implant abutments for single-tooth implants in canine and posterior regions: 3-year results. Clin Oral Implants Res 2009;20(8):802-8.
31. Abbo B, Razzoog ME, Vivas J, Sierraalta M. Resistance to dislodgement of zirconia copings cemented onto titanium abutments of different heights. J Prosthet Dent 2008;99(1):25-9.
32. Muhlemann S, Truninger TC, Stawarczyk B, Hammerle CH, Sailer I. Bending moments of zirconia and titanium implant abutments supporting all-ceramic crowns after aging. Clin Oral Implants Res 2014;25(1):74-81.
33. ISO. ISO 14801 Dentistry - Implants -Dynamic fatigue test for endosseous dental implants. 2007.
34. Lee CK, Karl M, Kelly JR. Evaluation of test protocol variables for dental implant fatigue research. Dent Mater 2009;25(11):1419-25.
35. Fraga S, Pereira GKR, Freitas M, et al. Loading frequencies up to 20Hz as an alternative to accelerate fatigue strength tests in a Y-TZP ceramic. Journal of the Mechanical Behavior of Biomedical Materials 2016;61:79-86.
36. Rocca GT, Sedlakova P, Saratti CM, et al. Fatigue behavior of resin-modified monolithic CAD-CAM RNC crowns and endocrowns. Dent Mater 2016;32(12):e338-e50.
37. Magne P, Schlichting LH, Maia HP, Baratieri LN. In vitro fatigue resistance of CAD/CAM composite resin and ceramic posterior occlusal veneers. J Prosthet Dent 2010;104(3):149-57.
38. Campos F, Valandro LF, Feitosa SA, et al. Adhesive Cementation Promotes Higher Fatigue Resistance to Zirconia Crowns. Oper Dent 2017;42(2):215-24.
39. Joda T, Huber S, Burki A, Zysset P, Bragger U. Influence of Abutment Design on Stiffness, Strength, and Failure of Implant-Supported Monolithic Resin Nano Ceramic (RNC) Crowns. Clin Implant Dent Relat Res 2014.
40. Costa AK, Borges AL, Fleming GJ, Addison O. The strength of sintered and adhesively bonded zirconia/veneer-ceramic bilayers. J Dent 2014;42(10):1269-76.
41. Costa AK, Kelly RD, Fleming GJ, Borges AL, Addison O. Laminated ceramics with elastic interfaces: a mechanical advantage? J Dent 2015;43(3):335-41.

ABSTRACT

PURPOSE: To evaluate the fatigue failure load of distinct lithium disilicate restoration designs cemented on a chairside titanium-base (Variobase™ for CEREC®, Straumann® LLC, USA) for restoring anterior implant restoration.

MATERIALS AND METHODS: Left maxillary incisor restoration was virtually designed in 3 groups (n=10; CTD: lithium disilicate crowns cemented on custom-milled titanium abutments; VMLD: monolithic full-contour lithium disilicate crowns cemented on titanium-base; and VCLD: lithium disilicate crowns cemented on lithium disilicate customized anatomic structures then cemented on titanium-base). The titanium-base was air-abraded with aluminum oxide particles, 50 μm at 2 bars. Subsequently the titanium-base was steamed, air-dried and a thin coat of silane (Monobond Plus, Ivoclar Vivadent®, USA). All ceramic components were surface treated with hydrofluoric acid etching gel, follow by silanized, and bonded with resin cement (Multilink Automix, Ivoclar Vivadent®, USA). Specimens were fatigued at 20 Hz, starting with a load of 100 N (×5000 cycles), followed by stepwise loading up to 1400 N at a maximum of 30,000 cycles each. The failure loads, number of cycles, and fracture analysis were recorded. Data were statistically analyzed using one-way ANOVA followed by pair-wise comparisons ($p < 0.05$). Kaplan-Meier survival plots and Weibull survival analyses were reported.

RESULT: For catastrophic fatigue failure load and total number of cycles for failure, VMLD (1260 N, 175231 cycles) was significantly higher than VCLD (1080 N, 139965 cycles) and CDT (1000 N, 133185 cycles). VMLD had higher Weibull modulus (11.6), demonstrating higher structural reliability.

CONCLUSIONS: VMLD performed the best fatigue behavior when compared with the

two other groups.

KEYWORDS: titanium, ceramic, lithium disilicate, implant abutment, chairside titanium-base, fatigue loading, stepwise

CURRICULUM VITAE

Peerapat Kaweewongprasert

Mar 2012	DDS, Srinakharinwirot University Bangkok, Thailand
Apr 2012 – Jun 2014	Full Time Prosthodontics Faculty Srinakharinwirot University Bangkok, Thailand
Jun 2017	Certificate in Prosthodontics Indiana University School of Dentistry Indianapolis, Indiana
Aug 2017	MSD (Dental Material) Indiana University School of Dentistry, Indianapolis, Indiana

Professional Organizations

Academy of Osseointegration (AO)
International Team for Implantology (ITI)
American College of Prosthodontists (ACP)
American Academy of Fixed Prosthodontics (AAFP)
American Academy of Maxillofacial Prosthetics (AAMP)
John F. Johnston Society (JFJ)
Thai Association of Dental Implantology (TADI)
The Thai Dental Association
The Thai Dental Council